



LTE-Advanced Signal Generation and Measurement Using SystemVue

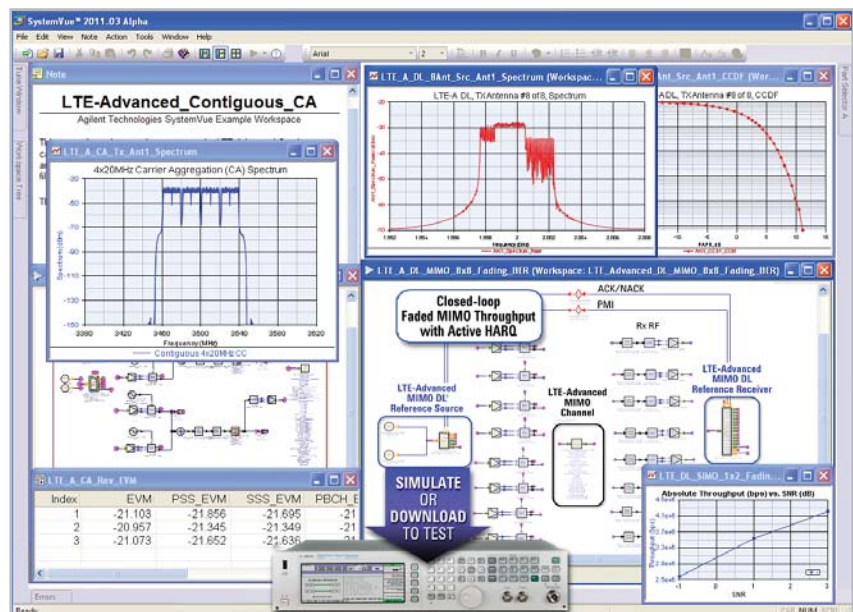
Application Note

Jinbiao Xu, Agilent EEsof EDA

Introduction

LTE-Advanced is specified as part of Release 10 of the 3GPP specifications and is now approved for 4G IMT-Advanced. This application note introduces key LTE-Advanced techniques, as well as how to use the Agilent SystemVue W1918 LTE-Advanced library to generate various downlink (DL) orthogonal frequency-division multiple access (OFDMA) and uplink (UL) clustered DFT-spread-OFDM (DFT-S-OFDM) signal sources with MIMO, and to measure closed-loop throughput.

This application note also introduces LTE-Advanced enhancements to the MIMO channel models, which are available as simulation model set called the W1715 SystemVue MIMO channel builder. This optional model set facilitates simulation-based MIMO over-the-air (OTA) testing using real, observed antenna patterns and standard MIMO fading models, and overcomes a key challenge for 8-layer MIMO system analysis and verification.



Agilent Technologies

LTE Overview

The LTE Release 8 downlink (DL) adopts orthogonal frequency-division multiplexing (OFDM) as its radio transmission scheme. The OFDM technique simplifies the receiver baseband processing to reduce terminal cost and power consumption. This is especially important taking into account the wide transmission bandwidths of LTE and even more so in combination with advanced DL multi-antenna transmission such as spatial multiplexing. The Release 8 uplink (UL) adopts DFT-S-OFDM, or Single-Carrier FDMA as its radio transmission scheme. SC-FDMA has smaller peak-to-average-power ratio (PAPR) than regular OFDM, thus enabling less-complex and/or higher-power terminals. Table 1 lists the major parameters of Release 8.

Table 1. Release 8 major parameters

Access scheme	DL	OFDMA
	UL	SC-FDMA
Bandwidth	1.4, 3, 5, 10, 15, 20 MHz	
Minimum TTI	1 ms	
Subcarrier spacing	15 kHz	
Cyclic prefix length	Short	4.7 us
	Long	16.7 us
Modulation	QPSK, 16-QAM, 64-QAM	
Spatial multiplexing	Single layer for UL per UE	
	Up to 4 layers for DL per UE	
	MU-MIMO supported for UL and DL	

Figure 3(a) shows the processing structure for the UL-SCH transport channel. Data arrives to the coding unit in the form of a maximum of one transport block every TTI. The following coding steps can be identified as:

- add CRC to the transport block;
- code block segmentation and code block CRC attachment;
- channel coding of data and control information;
- rate matching;
- code block concatenation;
- multiplexing of data and control information; and
- channel interleaver.

The baseband signal representing the physical UL shared channel is defined in terms of the following steps (Figure 3(b)):

- scrambling;
- modulation of scrambled bits to generate complex-valued symbols;
- transform precoding to generate complex-valued symbols;
- mapping of complex-valued symbols to resource elements; and
- generation of complex-valued time-domain SC-FDMA signals for each antenna port.

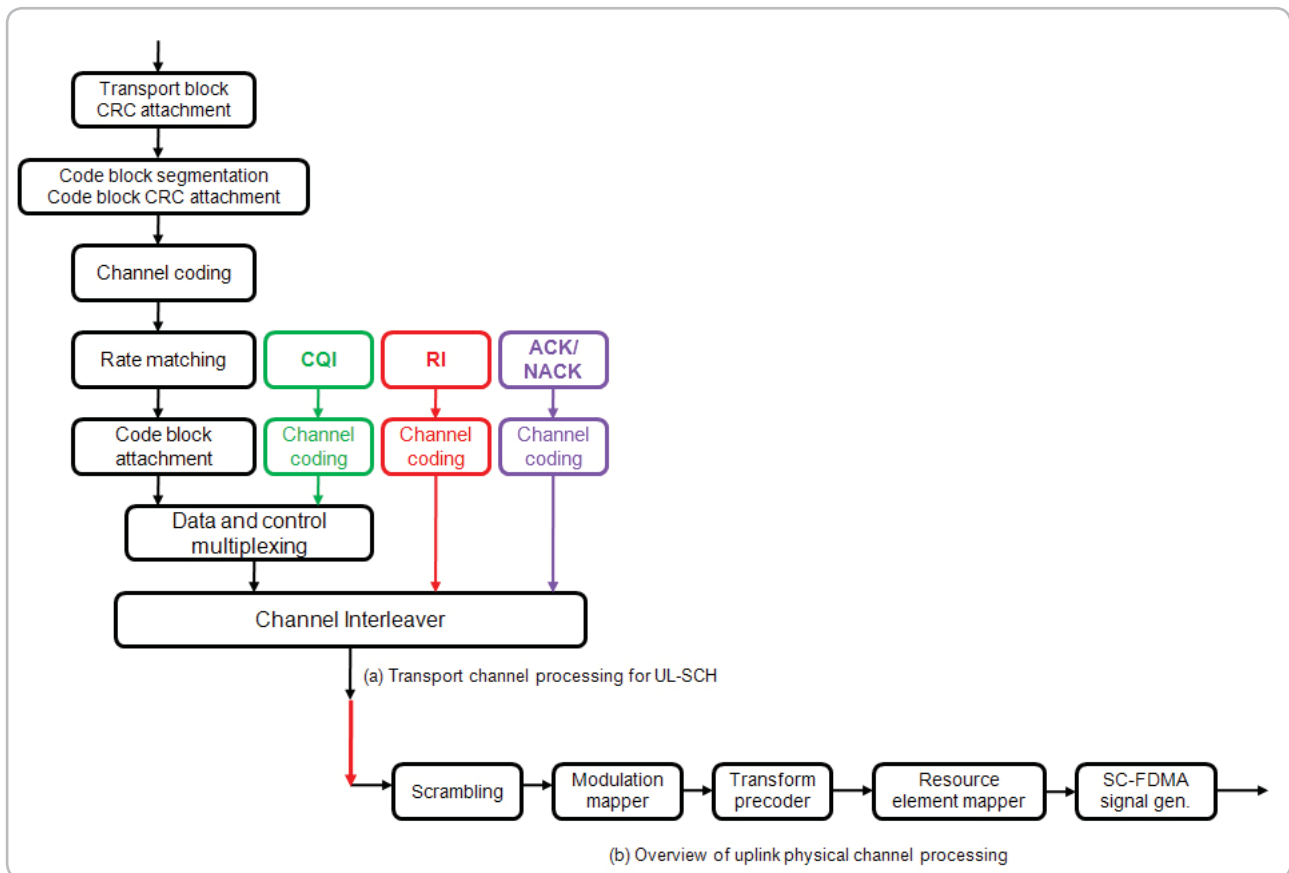


Figure 3. Uplink channel coding (TS 36.212) and physical channel processing (TS36.211) [ref 3,4, 16]

LTE supports system bandwidth from as small as 1.4 MHz up to 20 MHz, where the latter is needed to provide the highest data rates. LTE has the ability to use different UL and DL bandwidths, allowing spectrum usage tailored to different applications and regulatory requirements. LTE can operate in either paired or unpaired spectrum by supporting both Frequency-Division Duplex (FDD) and Time-Division Duplex (TDD) operation, using a single radio-access technology. Figure 1 shows the LTE frame structure for both FDD and TDD [14].

In the case of FDD, one carrier frequency is used for the uplink transmission (f_{UL}) and another carrier frequency for the downlink (f_{DL}). During a given LTE frame, UL and DL transmission can occur simultaneously within a cell, for any of 10 subframes of both UL or DL.

For TDD operation, there is only one carrier frequency, so UL and DL transmissions are always separated in time, as well as on a cell by cell basis. The guard period required for TDD operation is created by splitting one or two of the ten subframes in each radio frame into three special fields: a DL part (DwPTS), a guard period, and an UL part (UpPTS). The lengths of these special fields are configurable to allow for different deployment scenarios.

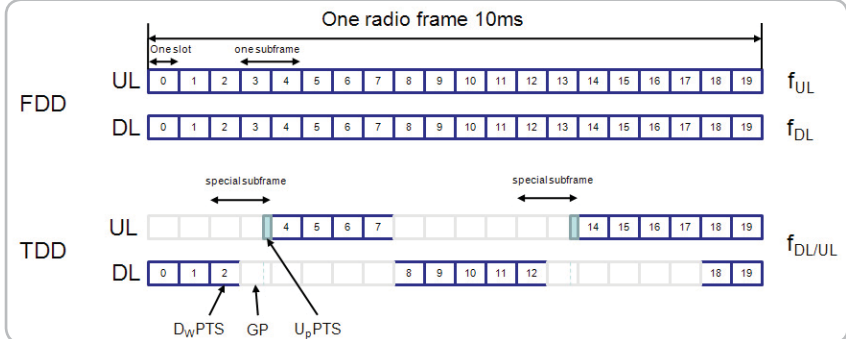


Figure 1. LTE FDD/TDD frame structure (Parkvall & Astely, pp 148 [14])

Multi-antenna transmission is a key feature in LTE Release 8. LTE supports the following 8 “transmission modes”, which are detailed in [15]. LTE-Advanced (Release 10) further introduces a Mode 9, discussed in a later section.

- Mode 1: Single antenna port, port 0
- Mode 2: Transmit diversity
- Mode 3: Large-delay CDD
- Mode 4: Closed-loop spatial multiplexing
- Mode 5: MU-MIMO
- Mode 6: Closed-loop spatial multiplexing, single layer
- Mode 7: Single antenna port, UE-specific RS (port 5)
- Mode 8: Single or dual-layer transmission with UE-specific RS (ports 7 and/or 8)

Figure 2(a) shows the processing structure for each transport block for the DL-SCH transport channels. Data arrives to the coding unit in the form of a maximum of two transport blocks every transmission time interval (TTI). The following coding steps can be identified for each transport block:

- add CRC to the transport block;
- code block segmentation and code block CRC attachment;
- channel coding;
- rate matching; and
- code block concatenation.

The baseband signal representing a DL physical channel is defined in terms of the following steps:

- scrambling of coded bits in each of the codewords to be transmitted on a physical channel;
- modulation of scrambled bits to generate complex-valued modulation symbols;
- mapping of the complex-valued modulation symbols onto one or several transmission layers;
- precoding of the complex-valued modulation symbols on each layer for transmission on the antenna ports;
- mapping of complex-valued modulation symbols for each antenna port to resource elements; and
- generation of complex-valued time-domain OFDM signals for each antenna port.

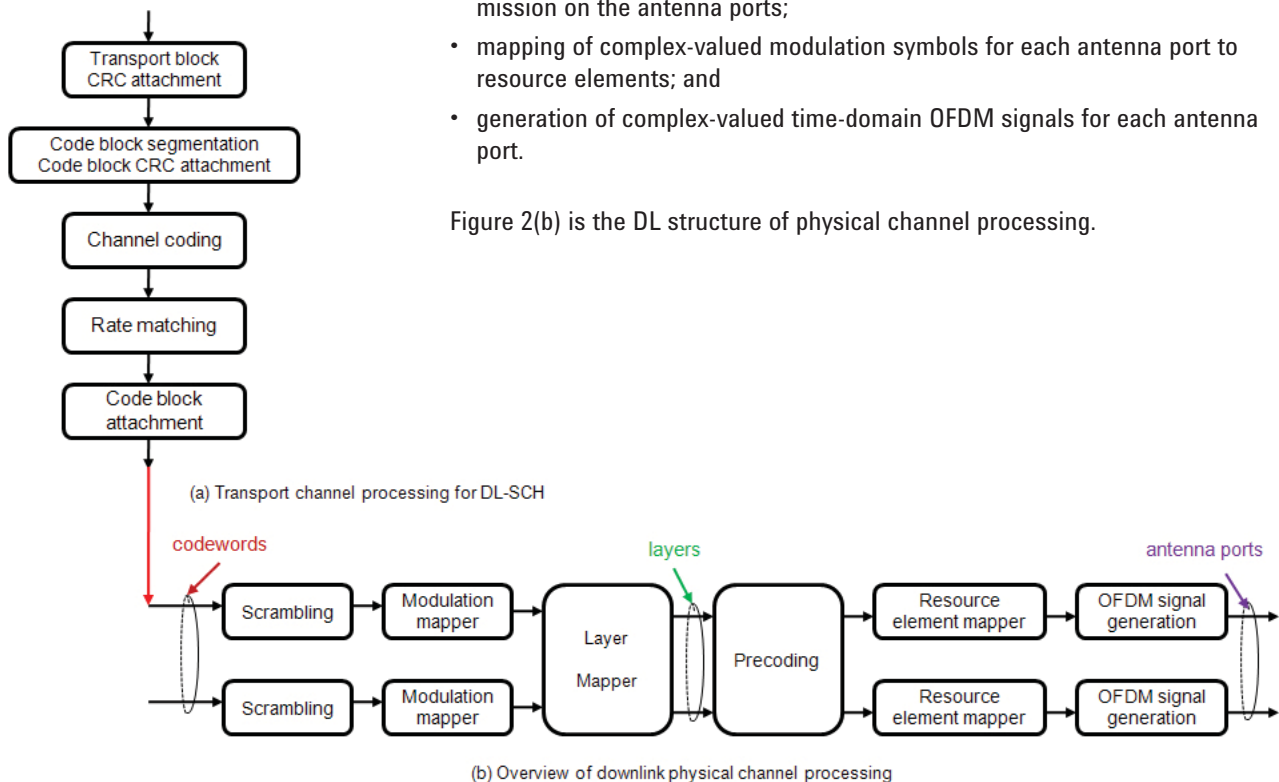


Figure 2. Downlink channel coding (TS 36.212) and physical channel processing (TS36.211) [ref 3,4, 16]

LTE-Advanced Requirements

The work by 3GPP to define a 4G radio interface technology candidate started in Release 9 with the study phase for LTE-Advanced. The requirements for LTE-Advanced are defined in 3GPP Technical Report (TR) 36.913, "Requirements for Further Advancements for E-UTRA (LTE-Advanced)." Major technical considerations include the following:

- Continual improvement to the LTE radio technology and architecture.
- Scenarios and performance requirements for interworking with legacy radio access technologies.
- Backward compatibility of LTE-Advanced with LTE. An LTE terminal should be able to work in an LTE-Advanced network and vice versa. Any exceptions will be considered by 3GPP.
- Advanced E-UTRA and Advanced E-UTRAN shall meet or exceed IMT-Advanced requirements.

Table 2 compares the spectral efficiency targets for LTE, LTE-Advanced and IMT-Advanced. Note that the peak rates for LTE-Advanced are substantially higher than the 4G requirements, which highlights a desire to increase peak performance in 4G LTE, although the average performance targets are closer to ITU requirements. It is worth noting that peak performance is often easier to demonstrate than average performance, because it only has to be met under ideal circumstances.

Table 2. Performance targets for LTE, LTE-Advanced and IMT-Advanced

Performance indicators		LTE Release 8	ITU-Advanced	LTE-Advanced Release 10
Peak data rate	DL	300 Mbps		1 Gbps
	UL	75 Mbps		500 Mbps
Peak spectrum efficiency [bps/Hz]	DL	15 [bps/Hz]	15 [bps/Hz]	30 [bps/Hz]
	UL	3.75 [bps/Hz]	6.75 [bps/Hz]	15 [bps/Hz]
Control plane latency		< 100 ms	100 ms	< 50 ms
User plane latency		< 5 ms	10 ms	< Rel – 8 LTE
Scalable bandwidth support		Up to 20 MHz	Up to 40 MHz	Up to 100 MHz
VoIP capacity		200 Active users per cell in 5 MHz	Up to 200 UEs per cell in 5 MHz	3 times higher than that in LTE
Cell spectrum efficiency	DL	2x2	1.69	2.4
		4x2	1.87	2.6
		4x4	2.67	3.7
	UL	1x2	0.735	1.2
		2x4	-	2
Cell edge spectrum efficiency	DL	2x2	0.05	0.07
		4x2	0.06	0.075
		4x4	0.08	0.12
	UL	1x2	0.024	0.04
		2x4	-	0.07

LTE-Advanced: New Features

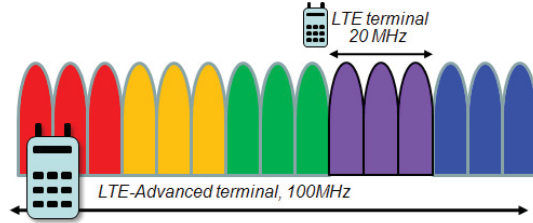
The new features of LTE-Advanced consist of both enhancements to LTE Release 8/9, as well as newer emerging technologies. Proposed solutions for achieving the performance targets for the LTE-Advanced radio interface are defined in 3GPP TR 36.814, “*Further Advancements for E-UTRA Physical Layer Aspects.*”

Enhancements relative to LTE Release 8/9	Emerging technologies
<ul style="list-style-type: none">• Carrier aggregation (CA)<ul style="list-style-type: none">◦ Contiguous and non-contiguous◦ Control channel design for UL/DL• Enhanced DL multiple access scheme• Enhanced UL multiple access scheme (Clustered SC-FDMA)• Enhanced DL MIMO transmission• Enhanced UL MIMO transmission	<ul style="list-style-type: none">• Relaying (multi-hop transmission)• Coordinated multipoint transmission and reception (CoMP)• Support for heterogeneous networks• LTE self-optimizing networks (SON)• HNB and HeNB mobility enhancements• CPE RF requirements

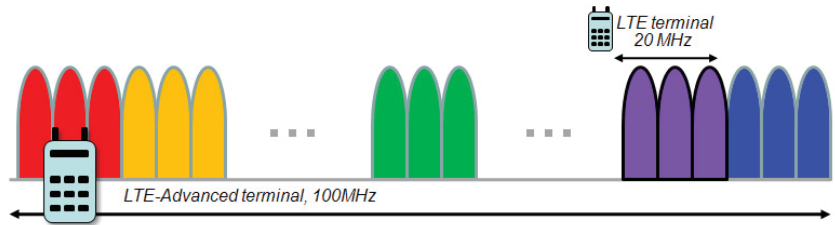
Several items in the emerging technologies section (above) are beyond the scope of LTE Release 10. In this application note, we only describe the LTE-Advanced features that are enhancements to Release 8/9, as implemented in the SystemVue W1918 LTE-Advanced library.

Carrier Aggregation (CA)

LTE Release 8 provides extensive support for deployment in a variety of spectrum allocations, ranging from 1.4 MHz to 20 MHz, in both paired and unpaired bands. Beyond 20 MHz, the only reasonable way to achieve LTE-Advanced’s highest target peak-throughput rates is to increase the transmission bandwidth, relative to Release 8. Therefore, LTE-Advanced specifies spectrum allocations of up to 100 MHz using “carrier aggregation”, where multiple component carriers are combined to provide the necessary bandwidth. It is possible to configure all component carriers that are LTE Release 8 compatible, at least when the aggregated numbers of component carriers in the UL and the DL are the same. However, not all component carriers are necessarily Release 8 compatible. Figure 4 shows carrier aggregation with contiguous carrier components and with non-contiguous carrier components.



(a) Contiguous carrier aggregation



(b) Non-contiguous carrier aggregation

Figure 4. Carrier aggregation (CA), with contiguous and non-contiguous carrier allocations

To insure the backward compatibility of eNB resource allocations, only minimum changes are required in the specifications if the scheduling, MIMO, Link Adaptation and HARQ are all performed in carrier groupings of 20MHz. For example, a user receiving information in the 100MHz bandwidth will need 5 receiver chains, one per each 20MHz block. Carrier aggregation is supported for both contiguous and non-contiguous component carriers, with each component carrier limited to a maximum of 110 Resource Blocks (RB) in the frequency domain (using LTE Release 8 numbering). It is possible to configure a UE to aggregate a different number of component carriers originating from the same eNB and possibly different bandwidths in the UL and the DL. Of course, in typical TDD deployments, the number of component carriers and the bandwidth of each component carrier in UL and DL will be the same.

The center frequency spacing of contiguously aggregated component carriers is in multiples of 300kHz. This is in order to be compatible with the 100 kHz frequency increments of Release 8 while at the same time preserving the orthogonality of subcarriers with a 15 kHz spacing. Depending on the aggregation scenario, the $N \times 300\text{kHz}$ spacing can be achieved by inserting a small number of unused subcarriers between contiguous component carriers.

Enhanced Downlink Multiple Access

In order to support carrier aggregation in the basestation (eNB), the DL should be updated. The DL uses OFDMA with a component carrier (CC) based structure. Figure 5 shows DL carrier aggregation with 4 contiguous carrier components. In DL multiple access, one transport block is mapped within one CC and parallel-type transmission for multi-CC transmission.

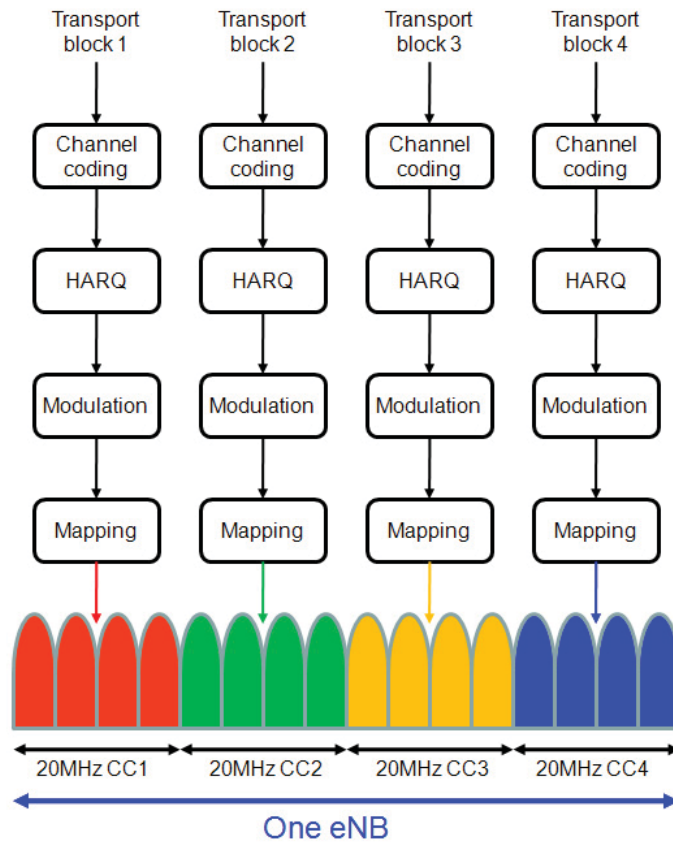


Figure 5. Carrier allocation in contiguous DL carrier aggregation [15]

This structure is in good alignment with Release 8 specifications; meanwhile, cross-carrier scheduling is also possible, where PDCCH on one carrier can relate to data on another carrier. DL control channels (such as PDCCH, PCFICH, and PHICH) are updated to support cross-carrier scheduling.

Cross-carrier scheduling can be configured on a per UE basis (as opposed to system-specific, or cell-specific basis) by adding a Carrier Indicator Field (CIF) to DCI.

The CIF is a fixed 3-bit field. Its location is fixed irrespective of DCI format size, if it is configured, and if the configuration is UE specific (e.g., also not system-specific or cell-specific). CIF always supports cross-carrier scheduling for DCI format 0, 1, 1A, 1B, 1D, 2, 2A, 2B in the UE-specific search space. It is not included in DCI format 0, 1A in the common search space when the CRC is scrambled by C-RNTI/SPS CRNTI.

Enhanced Uplink Multiple Access

The basic UL transmission scheme is single-carrier transmission (SC-FDMA) with a cyclic prefix to achieve inter-user uplink orthogonality and to enable efficient receiver-side equalization in the frequency domain. Frequency-domain generation of the signal, sometimes known as DFT-S-OFDM, is assumed and illustrated in Figure 6. This allows for a relatively high degree of commonality with the LTE DL OFDM scheme and the same parameters (such as clock frequency) can be reused.

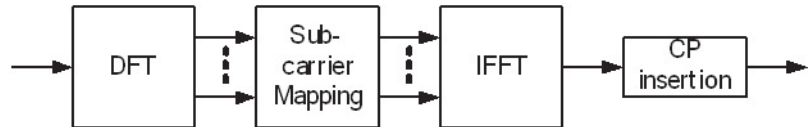


Figure 6. Transmitter scheme for SC-FDMA

LTE-Advanced enhances the UL multiple access scheme by adopting clustered DFT-S-OFDM. This scheme is similar to SC-FDMA but has the advantage that it allows non-contiguous (clustered) groups of subcarriers to be allocated for transmission by a single UE. This enables UL frequency-selective scheduling and better link performance. Clustered DFT-S-OFDM was chosen in preference to pure OFDM to avoid a significant increase in PAPR. It helps satisfy the requirement for increased UL spectral efficiency, while maintaining backward-compatibility with LTE. Please note that the only difference between SC-FDMA and clustered DFT-S-OFDM is in the subcarrier mapping block shown in Figure 6.

The subcarrier mapping of SC-FDMA determines which part of the spectrum is used for transmission by inserting a suitable number of zeros at the upper and/or lower end in Figure 8.

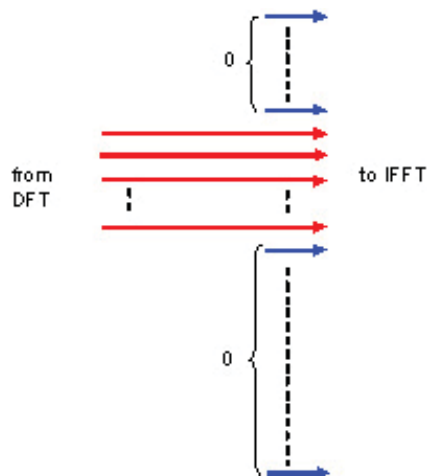


Figure 7. Subcarrier mapping for SC-FDMA

LTE Release 8 adopts contiguous PRB allocation (Figure 7). The number of allocated PRBs for a given user in a given subframe is expressed in multiples of 2, 3 and 5 for low complexity DFT implementation. Moreover, PUSCH and PUCCH cannot be transmitted simultaneously in LTE Release 8/9.

Figure 8 shows a diagram of subcarrier mapping between DFT and IFFT for clustered DFT-S-OFDM (LTE-Advanced). We can see non-contiguous subcarrier allocation is supported in clustered DFT-S-OFDM. In contrast, SC-FDMA supports contiguous subcarrier allocation. Clustered SC-FDMA transmission can provide more flexible scheduling than SC-FDMA in LTE.

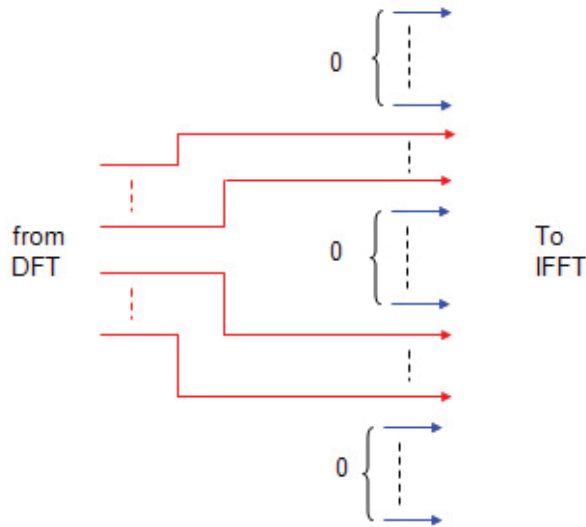


Figure 8. Mapping function of clustered SC-FDMA

In Release 10, UL provides hybrid multiple access of clustered DFT-S-OFDM and SC-FDMA to support contiguous and non-contiguous resource allocation. This hybrid multiple access enhances the flexibility and efficiency of resource allocation. It can be dynamically switched between Release 8 single cluster transmission and LTE Release 10 clustered transmission. Moreover, simultaneous PUCCH and PUSCH transmission will be supported in LTE-Advanced.

In order to reach the 500-Mb/s peak data rate for UL, while maintaining LTE's backward compatibility, LTE-Advanced adopts parallel multi-component carriers (CC) transmission to achieve wider bandwidth; something that was introduced in the previous carrier aggregation section. The UL bandwidth can be up to 100 MHz and there are up to five CCs in one UE. Figure 9 illustrates an example of UL with two contiguous CCs.

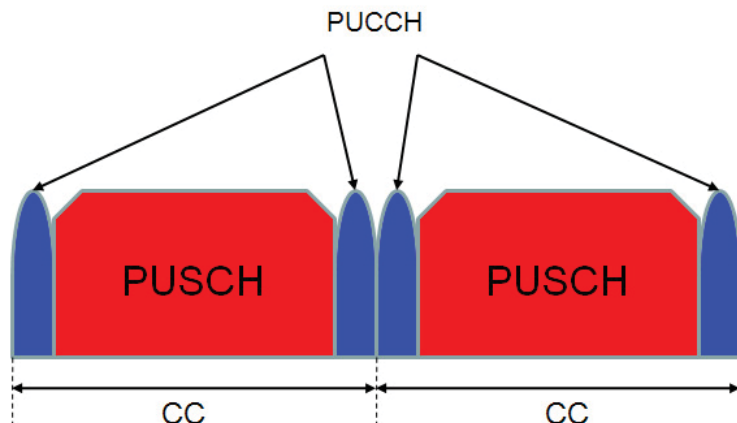


Figure 9. Two contiguous CCs in UE

From a UE perspective, there is only one transport block in LTE-Advanced (in the absence of spatial multiplexing) and one hybrid-ARQ entity per scheduled component carrier. Each transport block is mapped to a single component carrier. Of course, a UE may be scheduled over multiple component carriers simultaneously using carrier aggregation. Figure 10 shows an example of UL with four transport blocks.

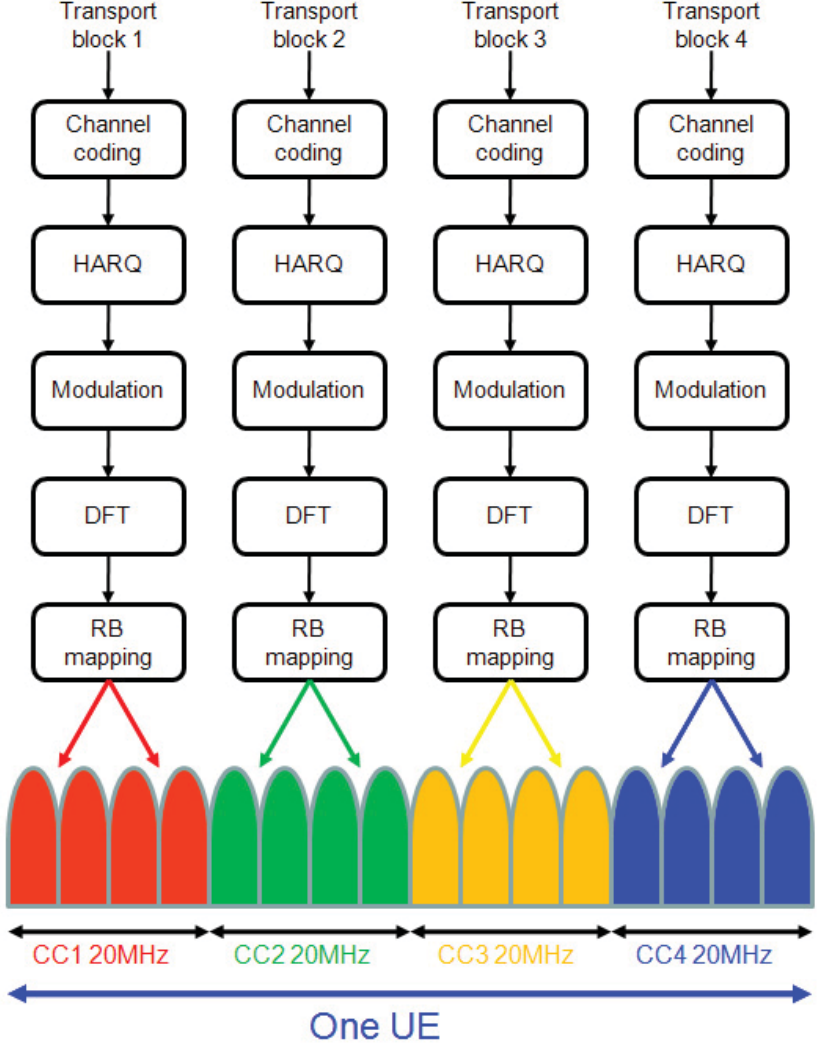


Figure 10. Four transport blocks CCs in one UE

When UL has several (up to 5) parallel multi-component carriers, there is one DFT per each component carrier for PUSCH transmission (see Figure 10) and the PUSCH transmission supports spatial multiplexing. There are also two types of resource allocations (frequency-contiguous and frequency non-contiguous) for PUSCH. In Figure 10, each transport block (1,2,3 or 4) can adopt clustered DFT-S-OFDM (non-contiguous subcarrier allocation) or SC-FDMA (contiguous subcarrier allocation, the same as the LTE UL).

The physical UL control channel, PUCCH, carries UL control information. There are six PUCCH formats (1/1a/1b/2/2a/2b) supported in Release 8. Formats 2a and 2b are supported for normal cyclic prefix only. In addition to the six PUCCH formats (1/1a/1b/2/2a/2b), LTE-Advanced has a new format 3 to convey a large number of ACK/NACK bits.

Table 3. Supported Physical UL Control Channel (PUCCH) formats

PUCCH format	Modulation scheme	Number of bits per subframe,
1	N/A	N/A
1a	BPSK	1
1b	QPSK	2
2	QPSK	20
2a	QPSK+BPSK	21
2b	QPSK+QPSK	22
3	QPSK	48

All ACK/NACK for a UE can be transmitted on PUCCH in the absence of PUSCH transmission. A single UE-specific UL CC is configured semi-statically for carrying PUCCH ACK/NACK. This method is used for assigning PUCCH resource(s) for a UE on the above single UL carrier in the case of carrier aggregation. In addition to ACK/NACK, a single UE-specific UL CC is configured semi-statically for carrying PUCCH SR and periodic CSI from a UE. Both simultaneous ACK/NACK on PUCCH transmission from 1 UE on multiple UL CCs and multiple simultaneous PUCCH transmission for ACK/NACK in multiple non-adjacent PRBs are not supported in LTE-A.

There are, at maximum, 10 ACK/NACK bits supported in the FDD system and an ACK/NACK payload size of up to 20 bits supported in the TDD system. When considering utilization of bundling, note that the FDD system does not support any carrier-domain bundling or spatial-domain bundling. TDD supports some bundling schemes (time-domain bundling or carrier-domain bundling) together with spatial domain bundling.

PUCCH format 1a/1b in Release 8 can support up to 2 ACK/NACK bits and PUCCH format 1b with channel selection can support up to 4 ACK/NACK bits. The new PUCCH format (PUCCH format 3) is introduced to support a larger number of ACK/NACK bits, which is based on DFT-S-OFDM.

The time and frequency resources that can be used by the UE to report CQI, PMI and RI are controlled by the eNB. CQI, PMI and RI reporting is periodic or aperiodic. A UE transmits periodic CQI/PMI, or RI reporting on PUCCH in subframes with no PUSCH allocation. A UE transmits periodic CQI/PMI or RI reporting on PUSCH in subframes with PUSCH allocation, where the UE uses the same PUCCH-based periodic CQI/PMI or RI reporting format on PUSCH.

A UE transmits aperiodic CQI/PMI and RI reporting on PUSCH if the conditions specified are met. For aperiodic CQI reporting, RI reporting is transmitted only if configured CQI/PMI/RI feedback type supports RI reporting. The CQI transmissions on PUCCH and PUSCH for various scheduling modes are summarized in Table 4.

Table 4. Physical channels for aperiodic or periodic CQI reporting

Scheduling Mode	Periodic CQI reporting channels	Aperiodic CQI reporting channels
Frequency non-selective	PUCCH	
Frequency selective	PUCCH	PUSCH

When the UL supports multi-component carriers in LTE-Advanced, we need to consider multiple CQIs on a single component carrier, multiple resources transmission joint coding and TDM to report CQI/PMI/RI in periodic PUCCH or aperiodic PUSCH. Note that at the time of this writing, the decision as to which enhanced UL features will make it into the Release 10 specifications is still under discussion.

Figure 11(a) shows the processing structure for the UL-SCH transport channel on one UL cell. Data arrives to the coding unit in the form of a maximum of two transport blocks every TTI per UL cell. The following coding steps can be identified for each transport block of the UL cell:

- add CRC to the transport block;
- code block segmentation and code block CRC attachment;
- channel coding of data and control information;
- rate matching;
- code block concatenation;
- multiplexing of data and control information; and
- channel interleaver.

Figure 11(b) shows the baseband signal processing of UL_SCH in LTE_Advanced. The baseband signal representing the physical UL shared channel is defined in terms of the following steps:

- scrambling;
- modulation of scrambled bits to generate complex-valued symbols;
- mapping of the complex-valued modulation symbols onto one or several transmission layers;
- transform precoding to generate complex-valued symbols;
- precoding of the complex-valued symbols;
- mapping of precoded complex-valued symbols to resource elements; and
- generation of complex-valued time-domain SC-FDMA signals for each antenna port.

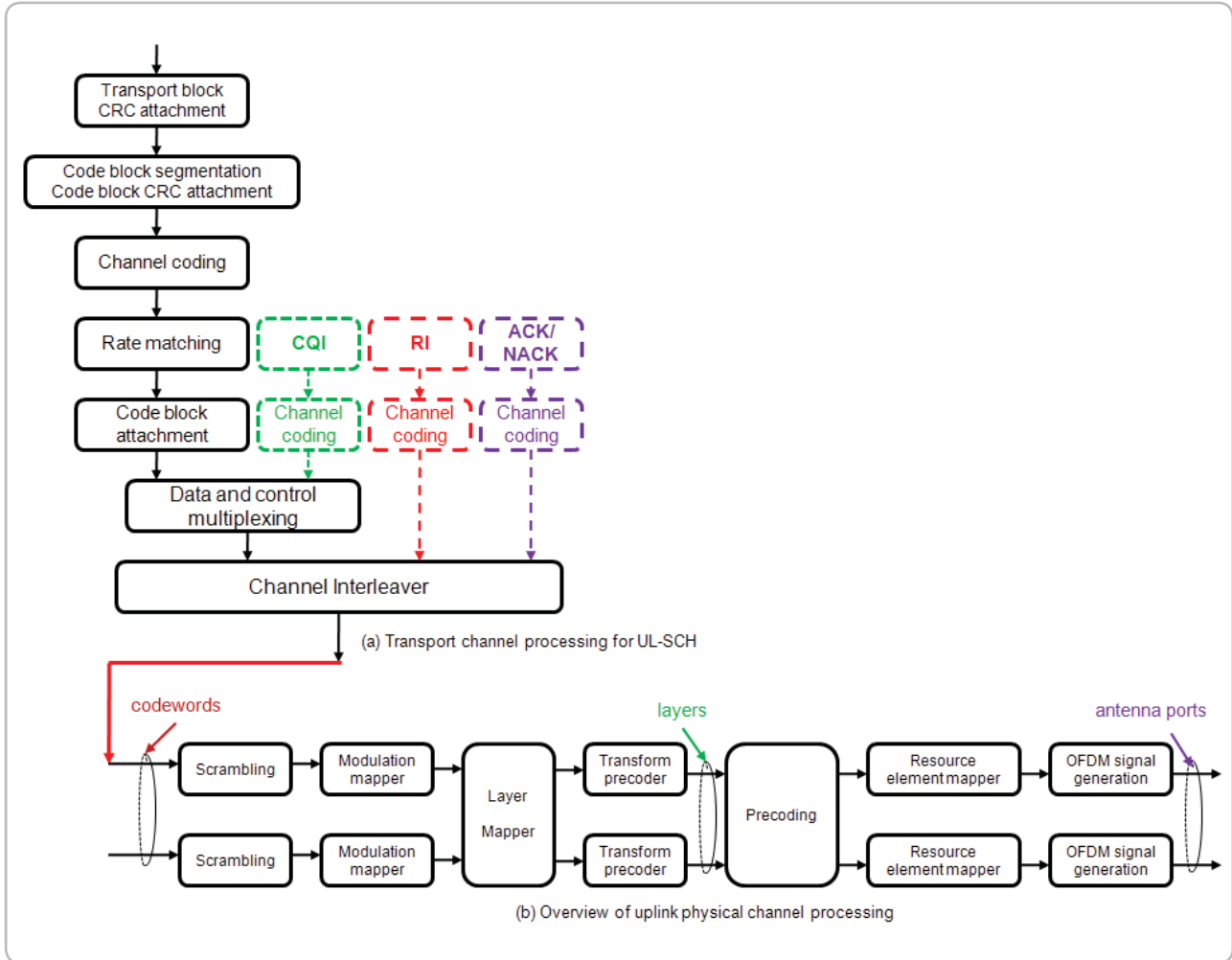


Figure 11. Uplink channel coding (TS 36.212) and physical channel processing (TS36.211) [ref 3,4, 16]

Comparing Figures 3 and 11, we can see the difference in the channel coding and physical channel processing between LTE and LTE-Advanced.

Enhanced Downlink MIMO Transmission

In addition to wider bandwidth, LTE-Advanced is also expected to provide higher data rates and improved system performance. It will do this by further extending the support for multi-antenna transmission compared to the first release of LTE. For the DL, up to eight layers can be transmitted using an 8x8 antenna configuration. This allows for a peak spectral efficiency exceeding the requirement of 30 bits/s/Hz and implies a possibility for data rates beyond 1 Gbit/s in a 40-MHz bandwidth and even higher data rates with wider bandwidth. First, let us introduce the five types of DL reference signals are defined in Release 10. They include:

1. cell-specific reference signals (CRS);
2. MBSFN reference signals;
3. UE-specific reference signals (DMRS);
4. positioning reference signals (PRS); and
5. CSI reference signals (CSI-RS);

Cell-specific RS is transmitted in each physical antenna port. It is used for both demodulation and measurement purpose. Its pattern design ensures channel estimation accuracy. LTE-Advanced eNB should always support LTE UE as well. This CRS is also used for LTE-Advanced UEs to detect PCFICH, PHICH, PDCCH, PBCH, and PDSCH (transmit diversity only).

UE-specific reference signals are supported for transmission of PDSCH and are transmitted on antenna port(s) $0, 1, \dots, N-1$, where N is the number of layers used for transmission of the PDSCH. UE-specific DMRS can be precoded, and supports non-codebook-based precoding. It will enable application of enhanced multi-user beamforming, such as zero forcing (ZF) for 4x2 MIMO. The DMRS pattern for higher numbers of layers is extended from a 2-layer format for transmission mode 8 in Release 9.

The CSI reference signal is transmitted in each physical antenna port or virtualized antenna port and is used for measurement purposes only. Its channel estimation accuracy can be relatively lower than DMRS.

In Release 8, CRS is used for both demodulation and measurement. According to CRS, precoding information can be informed to a UE, physical antenna ports can be seen by a UE and CRS power boosting is necessary for supporting various type of geometry UE. The LTE DL MIMO transmission is based on CRS. Figure 12 shows the CRS-based structure.

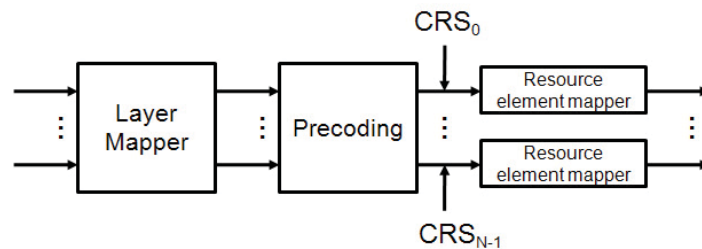


Figure 12. CRS-based MIMO scheme in LTE

In LTE-Advanced, DL MIMO transmission is based on DMRS. Figure 13 shows the DMRS-based structure. Here, DMRS is used for demodulation and CSI-RS is used for measurement, respectively. Precoding information is not needed for demodulation. Virtual antenna ports (stream) can be seen by a UE. Precoding gain can be exploited for channel estimation and DMRS power boosting may not be needed.

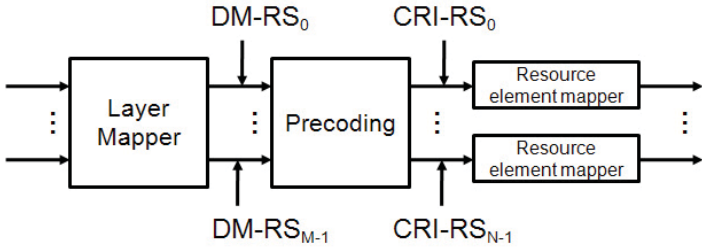


Figure 13. DMRS-based MIMO scheme in LTE-Advanced

(Release 8 supports eight transmission modes, previously introduced in the “LTE Overview” introduction. LTE-Advanced adds a new transmission Mode 9 “multi-layer transmission mode” to support closed-loop SU-MIMO up to rank 8. In this mode, Release 10 DMRS will be used for demodulation and it can support up to eight-layer transmission. The precoder index is not necessary to inform and the DL precoder is not specified. Consequently, flexible precoder usage is possible in the eNB design due to the precoded DMRS based transmission. In order to support Mode 9 transmission, the DCI format 2C is defined.

LTE Release 10 also reuses the Release 8 transmit diversity (TD) scheme with cell-specific reference signals (CRS) in a normal subframe to keep backwards compatibility.

Corresponding to the LTE-Advanced DL MIMO upgrade, the feedback (CQI/PMI/RI) also must be updated.

Enhanced Uplink MIMO Transmission

LTE-Advanced will include spatial multiplexing of up to four layers for the UL. With four-layer transmission in the UL, a peak UL spectral efficiency exceeding 15 bits/s/Hz can be achieved. Many of the techniques employed for DL spatial multiplexing are already in Release 8. For example, codebook-based and non-codebook-based channel-dependent precoding can be considered to not only enhance peak rates, but also cell-edge data rates.

In UL spatial multiplexing mode, codeword-to-layer mapping is same as the DL codeword-to-layer mapping for 2 TX and 4 TX defined in Release 8. The codebook design is based on precoding. There is an independent codebook design for different ranks and a single wideband TPMI per UL component carrier.

The codebook size of 2 transmit antennas is less than 8 and there is a 3-bit codebook for 2 TX. The codebook size of 4 transmit antennas is less than 64 and there is a 6-bit codebook for 4 TX.

For UL spatial multiplexing with two transmit antennas, the 3-bit precoding codebook is defined in Table 5. The codebook size of Rank 1 ($v=1$) is 6 and of Rank 2 ($v=2$) is 1. Note that the codebook index 4 and 5 of Rank 1 are antenna selection precoders.

Table 5. Codebook for 2 transmission antennas

V =	Number of layers	
	V = 1	V = 2
0	$\sqrt{\frac{1}{2}} \begin{bmatrix} 1 \\ 1 \end{bmatrix}$	$\sqrt{\frac{1}{2}} \begin{bmatrix} 1 & 0 \\ 1 & 1 \end{bmatrix}$
1	$\sqrt{\frac{1}{2}} \begin{bmatrix} 1 \\ -1 \end{bmatrix}$	-
2	$\sqrt{\frac{1}{2}} \begin{bmatrix} 1 \\ j \end{bmatrix}$	-
3	$\sqrt{\frac{1}{2}} \begin{bmatrix} 1 \\ -j \end{bmatrix}$	-
4	$\sqrt{\frac{1}{2}} \begin{bmatrix} 1 \\ 0 \end{bmatrix}$	-
5	$\sqrt{\frac{1}{2}} \begin{bmatrix} 0 \\ 1 \end{bmatrix}$	-

For UL spatial multiplexing with four transmit antennas, a 6-bit precoding codebook is used. The subset of the precoding codebook used for Rank-1 (1-layer) transmission is defined in Table 6. The codebook size of Rank 1 ($v=1$) is 24. Note that the codebook indexes from 16 to 23 are antenna selection precoders and indexes from 0 to 15 are constant modulus.

Table 6. Codebook for 4 transmission antennas with Rank-1 ($V = 1$)

Codebook Index	Number of layers $V = 1$							
0 - 7	$\frac{1}{2} \begin{bmatrix} 1 \\ 1 \\ 1 \\ -1 \end{bmatrix}$	$\frac{1}{2} \begin{bmatrix} 1 \\ 1 \\ j \\ j \end{bmatrix}$	$\frac{1}{2} \begin{bmatrix} 1 \\ 1 \\ -1 \\ -1 \end{bmatrix}$	$\frac{1}{2} \begin{bmatrix} 1 \\ 1 \\ -j \\ j \end{bmatrix}$	$\frac{1}{2} \begin{bmatrix} 1 \\ j \\ 1 \\ j \end{bmatrix}$	$\frac{1}{2} \begin{bmatrix} 1 \\ j \\ j \\ -1 \end{bmatrix}$	$\frac{1}{2} \begin{bmatrix} 1 \\ j \\ 1 \\ -j \end{bmatrix}$	$\frac{1}{2} \begin{bmatrix} 1 \\ j \\ -j \\ 1 \end{bmatrix}$
8 - 15	$\frac{1}{2} \begin{bmatrix} 1 \\ -1 \\ 1 \\ 1 \end{bmatrix}$	$\frac{1}{2} \begin{bmatrix} 1 \\ -1 \\ j \\ -j \end{bmatrix}$	$\frac{1}{2} \begin{bmatrix} 1 \\ -1 \\ -1 \\ 1 \end{bmatrix}$	$\frac{1}{2} \begin{bmatrix} 1 \\ -1 \\ -j \\ j \end{bmatrix}$	$\frac{1}{2} \begin{bmatrix} 1 \\ -j \\ 1 \\ -j \end{bmatrix}$	$\frac{1}{2} \begin{bmatrix} 1 \\ -j \\ j \\ -1 \end{bmatrix}$	$\frac{1}{2} \begin{bmatrix} 1 \\ -j \\ -1 \\ j \end{bmatrix}$	$\frac{1}{2} \begin{bmatrix} 1 \\ -j \\ -j \\ 1 \end{bmatrix}$
16 - 23	$\frac{1}{2} \begin{bmatrix} 1 \\ 0 \\ 1 \\ 0 \end{bmatrix}$	$\frac{1}{2} \begin{bmatrix} 1 \\ 0 \\ -1 \\ 0 \end{bmatrix}$	$\frac{1}{2} \begin{bmatrix} 1 \\ 0 \\ j \\ 0 \end{bmatrix}$	$\frac{1}{2} \begin{bmatrix} 1 \\ 0 \\ -j \\ 0 \end{bmatrix}$	$\frac{1}{2} \begin{bmatrix} 0 \\ 1 \\ 0 \\ 1 \end{bmatrix}$	$\frac{1}{2} \begin{bmatrix} 0 \\ 1 \\ 0 \\ -1 \end{bmatrix}$	$\frac{1}{2} \begin{bmatrix} 0 \\ 1 \\ j \\ 0 \end{bmatrix}$	$\frac{1}{2} \begin{bmatrix} 0 \\ 1 \\ -j \\ 0 \end{bmatrix}$

The baseline for the subset of the precoding codebook used for Rank-2 transmission is defined in Table 7. The codebook size of Rank 2 ($v=2$) is 16 and the codebook is CM-preserving matrices and QPSK alphabet.

Table 7. Codebook for 4 transmission antennas with Rank-2 ($V = 2$)

Codebook Index	Number of layers $V = 2$			
0 - 3	$\frac{1}{2} \begin{bmatrix} 1 & 0 \\ 1 & 0 \\ 0 & 1 \\ 0 & -j \end{bmatrix}$	$\frac{1}{2} \begin{bmatrix} 1 & 0 \\ 1 & 0 \\ 0 & 1 \\ 0 & j \end{bmatrix}$	$\frac{1}{2} \begin{bmatrix} 1 & 0 \\ -j & 0 \\ 0 & 1 \\ 0 & 1 \end{bmatrix}$	$\frac{1}{2} \begin{bmatrix} 1 & 0 \\ -j & 0 \\ 0 & 1 \\ 0 & -1 \end{bmatrix}$
4 - 7	$\frac{1}{2} \begin{bmatrix} 1 & 0 \\ -1 & 0 \\ 0 & 1 \\ 0 & -j \end{bmatrix}$	$\frac{1}{2} \begin{bmatrix} 1 & 0 \\ -1 & 0 \\ 0 & 1 \\ 0 & j \end{bmatrix}$	$\frac{1}{2} \begin{bmatrix} 1 & 0 \\ j & 0 \\ 0 & 1 \\ 0 & 1 \end{bmatrix}$	$\frac{1}{2} \begin{bmatrix} 1 & 0 \\ j & 0 \\ 0 & 1 \\ 0 & -1 \end{bmatrix}$
8 - 11	$\frac{1}{2} \begin{bmatrix} 1 & 0 \\ 0 & 1 \\ 1 & 0 \\ 0 & 1 \end{bmatrix}$	$\frac{1}{2} \begin{bmatrix} 1 & 0 \\ 0 & 1 \\ 1 & 0 \\ 0 & -1 \end{bmatrix}$	$\frac{1}{2} \begin{bmatrix} 1 & 0 \\ 0 & 1 \\ -1 & 0 \\ 0 & 1 \end{bmatrix}$	$\frac{1}{2} \begin{bmatrix} 1 & 0 \\ 0 & 1 \\ -1 & 0 \\ 0 & -1 \end{bmatrix}$
12-15	$\frac{1}{2} \begin{bmatrix} 1 & 0 \\ 0 & 1 \\ 0 & 1 \\ 1 & 0 \end{bmatrix}$	$\frac{1}{2} \begin{bmatrix} 1 & 0 \\ 0 & 1 \\ 0 & -1 \\ 1 & 0 \end{bmatrix}$	$\frac{1}{2} \begin{bmatrix} 1 & 0 \\ 0 & 1 \\ 0 & 1 \\ -1 & 0 \end{bmatrix}$	$\frac{1}{2} \begin{bmatrix} 1 & 0 \\ 0 & 1 \\ 0 & -1 \\ -1 & 0 \end{bmatrix}$

The subset of the precoding codebook used for Rank-3 (3-layer) transmission is defined in Table 8. The codebook size of Rank 3 ($v=3$) is 12. The codebook is CM-preserving matrices and BPSK alphabet.

Table 8. Codebook for 4 transmission antennas with Rank-3 ($V = 3$)

Codebook Index	Number of layers $V = 3$			
0 - 3	$\frac{1}{2} \begin{bmatrix} 1 & 0 & 0 \\ 1 & 0 & 0 \\ 0 & 1 & 0 \\ 0 & 0 & 1 \end{bmatrix}$	$\frac{1}{2} \begin{bmatrix} 1 & 0 & 0 \\ -1 & 0 & 0 \\ 0 & 1 & 0 \\ 0 & 0 & 1 \end{bmatrix}$	$\frac{1}{2} \begin{bmatrix} 1 & 0 & 0 \\ 0 & 1 & 0 \\ 1 & 0 & 0 \\ 0 & 0 & 1 \end{bmatrix}$	$\frac{1}{2} \begin{bmatrix} 1 & 0 & 0 \\ 0 & 1 & 0 \\ -1 & 0 & 0 \\ 0 & 0 & 1 \end{bmatrix}$
4 - 7	$\frac{1}{2} \begin{bmatrix} 1 & 0 & 0 \\ 0 & 1 & 0 \\ 0 & 0 & 1 \\ 1 & 0 & 0 \end{bmatrix}$	$\frac{1}{2} \begin{bmatrix} 1 & 0 & 0 \\ 0 & 1 & 0 \\ 0 & 0 & 1 \\ -1 & 0 & 0 \end{bmatrix}$	$\frac{1}{2} \begin{bmatrix} 0 & 1 & 0 \\ 1 & 0 & 0 \\ 1 & 0 & 0 \\ 0 & 0 & 1 \end{bmatrix}$	$\frac{1}{2} \begin{bmatrix} 0 & 1 & 0 \\ 1 & 0 & 0 \\ -1 & 0 & 0 \\ 0 & 0 & 1 \end{bmatrix}$
8 - 11	$\frac{1}{2} \begin{bmatrix} 0 & 1 & 0 \\ 1 & 0 & 0 \\ 0 & 0 & 1 \\ 1 & 0 & 0 \end{bmatrix}$	$\frac{1}{2} \begin{bmatrix} 0 & 1 & 0 \\ 1 & 0 & 0 \\ 0 & 0 & 1 \\ -1 & 0 & 0 \end{bmatrix}$	$\frac{1}{2} \begin{bmatrix} 0 & 1 & 0 \\ 0 & 0 & 1 \\ 1 & 0 & 0 \\ 1 & 0 & 0 \end{bmatrix}$	$\frac{1}{2} \begin{bmatrix} 0 & 1 & 0 \\ 0 & 0 & 1 \\ 1 & 0 & 0 \\ -1 & 0 & -0 \end{bmatrix}$

The precoding codebook used for Rank-4 (4-layer) transmission is a single identity matrix, as shown in Table 9.

Table 9. Codebook for 4 transmission antennas with Rank-4 ()

Codebook Index	Number of layers $V = 4$
0	$\frac{1}{2} \begin{bmatrix} 1 & 0 & 0 & 0 \\ 0 & 1 & 0 & 0 \\ 0 & 0 & 1 & 0 \\ 0 & 0 & 0 & 1 \end{bmatrix}$

In UL, transmit diversity is also adopted. PUCCH supports transmit diversity. Its transmit diversity is named Spatial Orthogonal-Resource Transmit Diversity (SORTD). Its performance is quite good in most cases. But, it requires 2x resources compared to what is required without transmit diversity.

LTE-Advanced/IMT-Advanced Channel Model

The ITU-R IMT-Advanced channel model is a geometry-based stochastic model that is based on WINNER II. It does not explicitly specify the locations of the scatterers, but rather the directions of the rays, like the well-known spatial channel model (SCM). Geometry-based modeling of the radio channel enables separation of propagation parameters and antennas.

The channel parameters for individual snapshots are determined stochastically based on statistical distributions extracted from channel measurements. Antenna geometries and radiation patterns can be defined properly by model user. Channel realizations are generated through the application of the geometrical principle by summing contributions of rays (plane waves) with specific small-scale parameters like delay, power, angle-of-arrival (AoA), and angle-of-departure (AoD). Superposition results to correlation between antenna elements and temporal fading with geometry-dependent Doppler spectrum.

A number of rays constitute a cluster. In the terminology of this document, we equate the cluster with a propagation path diffused in space, either or both in delay and angle domains. Elements of the MIMO channel (e.g., antenna arrays at both link ends and propagation paths), are illustrated in Figure 14. The generic MIMO channel model is applicable for all scenarios (indoor, urban and rural).

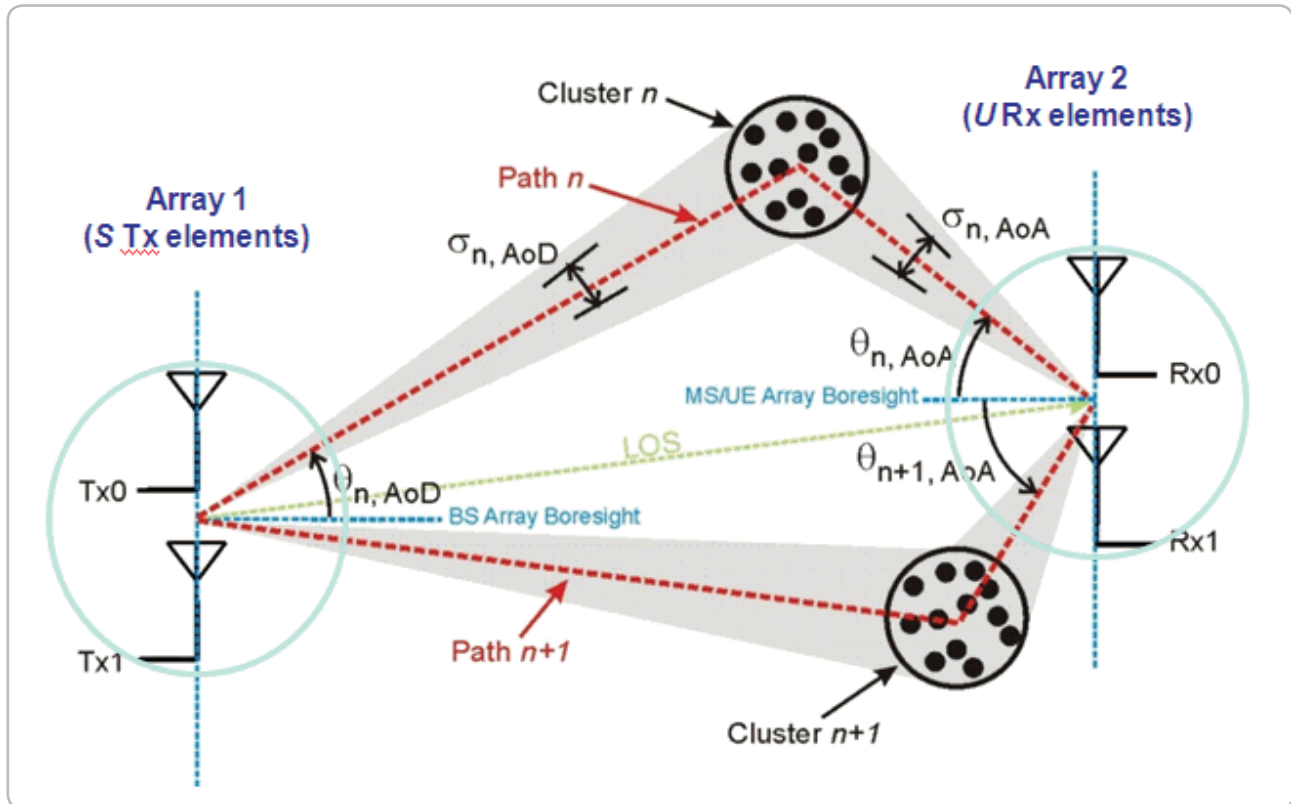


Figure 14. Representation of the MIMO channel

The time-variant impulse response matrix of the U x S MIMO channel is given by:

$$\mathbf{H}(t; \tau) = \sum_{n=1}^N \mathbf{H}_n(t; \tau) \quad (1)$$

where t is time, τ is delay, N is the number of paths (clusters), and n is path index. It is composed of the antenna array response matrices F_{tx} and F_{rx} for the transmitter (Tx) and the receiver (Rx), respectively, and the dual-polarized propagation channel response matrix h_n for cluster n as follows:

$$\mathbf{H}_n(t; \tau) = \iint \mathbf{F}_{rx}(\phi) \mathbf{h}_n(t; \tau, \phi, \varphi) \mathbf{F}_{tx}^T(\phi) d\phi d\varphi \quad (2)$$

The channel from the Tx antenna element s to Rx element u for cluster n is expressed as:

$$\begin{aligned} H_{u,s,n}(t; \tau) = & \sum_{m=1}^M \begin{bmatrix} F_{rx,u,V}(\phi_{n,m}) \\ F_{rx,u,H}(\phi_{n,m}) \end{bmatrix}^T \begin{bmatrix} \alpha_{n,m,VV} & \alpha_{n,m,VH} \\ \alpha_{n,m,HV} & \alpha_{n,m,HH} \end{bmatrix} \begin{bmatrix} F_{tx,s,V}(\phi_{n,m}) \\ F_{tx,s,H}(\phi_{n,m}) \end{bmatrix} \\ & \times \exp(j2\pi\lambda_0^{-1}(\bar{\phi}_{n,m} \cdot \bar{r}_{rx,u})) \exp(j2\pi\lambda_0^{-1}(\bar{\phi}_{n,m} \cdot \bar{r}_{tx,s})) \\ & \times \exp(j2\pi\nu_{n,m}t) \delta(\tau - \tau_{n,m}) \end{aligned}$$

where $F_{rx,u,V}$ and $F_{rx,u,H}$ are the antenna element u field patterns for vertical and horizontal polarizations, respectively, $\alpha_{n,m,VV}$ and $\alpha_{n,m,VH}$ are the complex gains of vertical-to-vertical and horizontal-to-vertical polarizations of ray n,m , respectively, λ_0 is the wave length of the carrier frequency, $\phi_{n,m}$ is the AoD unit vector, $\varphi_{n,m}$ is the AoA unit vector, $r_{tx,s}$ and $r_{rx,u}$ are the location vectors of element s and u , respectively, and $\nu_{n,m}$ is the Doppler frequency component of ray n,m . If the radio channel is modeled as dynamic, all of the above mentioned small-scale parameters are time variant (they are functions of t).

The generic channel model is a double-directional geometry-based stochastic model. It is a system-level model in the sense that it is employed, for example, in the SCM model. It can describe an unlimited number of propagation environment realizations for single or multiple radio links, for all the defined scenarios and for arbitrary antenna configurations, with one mathematical framework by different parameter sets. The generic channel model is a stochastic model with two (or three) levels of randomness. Figure 15 shows the overview of the channel model creation. The first stage consists of two steps. First, the propagation scenario is selected. Then, the network layout and the antenna configuration are determined. In the second stage, large-scale and small-scale parameters are defined. In the third stage, channel impulse responses (ChIRs) are calculated. Note that the antenna pattern should be input to ChIR generation to calculate the correlation matrix.

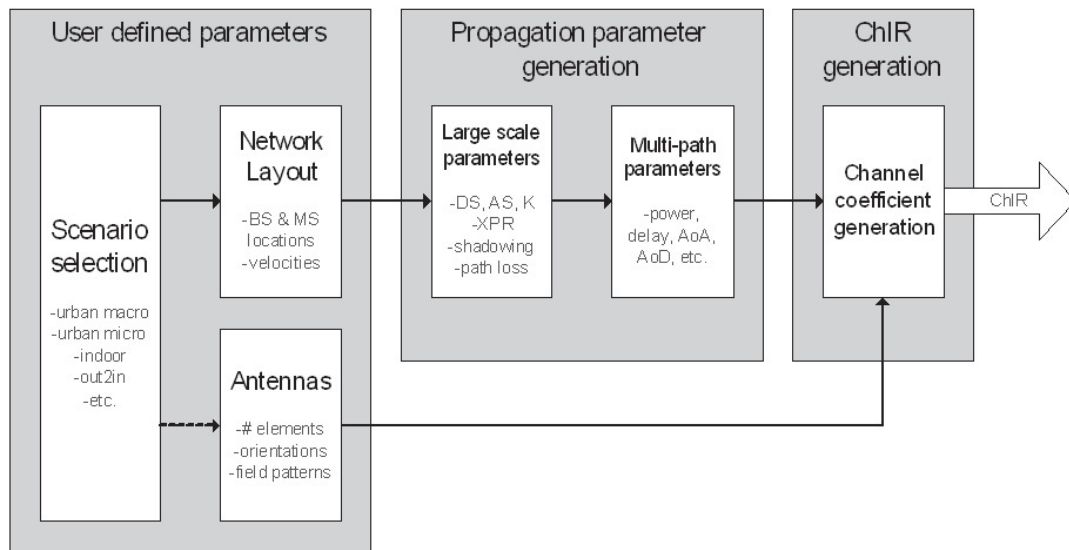


Figure 15. Process for creating generic channel model [TR 36.814]

The channel realizations are obtained by a step-wise procedure illustrated in Figure 16. It should be noted that the geometric description covers arrival angles from the last bounce scatterers and respectively, departure angles to the first scatterers interacted from the transmitting side. The propagation between the first and the last interaction is not defined. Thus, this approach can model also multiple interactions with the scattering media. This indicates also that the delay of a multipath component cannot be determined by the geometry. In the following steps, DL is assumed. For UL, arrival and departure parameters have to be swapped.

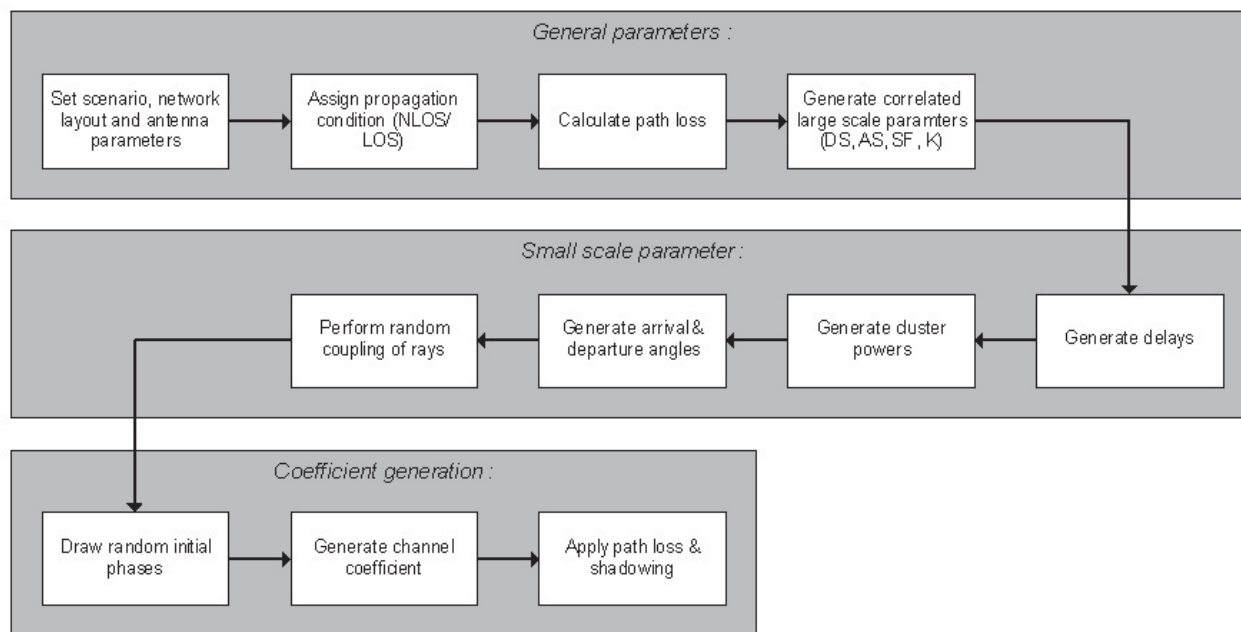


Figure 16. Procedure for generating channel coefficient [TR 36.814]

Introducing the LTE-Advanced baseband reference library for SystemVue

For the remainder of this application note, the SystemVue W1918 LTE-Advanced baseband verification library will be discussed. SystemVue is Agilent's electronic design automation (EDA) environment for electronic system level design, focused on the physical layer (PHY) of wireless communication systems. SystemVue enables system architects and algorithm developers to combine signal processing innovations with accurate RF system modeling, interaction with test equipment, and algorithm-level reference IP and applications. The W1918 LTE-Advanced library is an option to SystemVue that provides > 100 reference models, coded sources and receivers, and testbenches for both 3GPP Release 8 and Release 10.

The sections below describe some of the highly-parameterized sources that are new for Release 10. They can be used as open block diagram references for algorithm developers, or to provide customizable test vectors for download to test equipment for hardware verification. Of particular note is SystemVue's ability to simulate multi-channel MIMO scenarios that may be less convenient to configure as actual hardware measurements, thus providing a simulation-based alternative for early algorithmic and functional verification.

SystemVue LTE-Advanced Downlink MIMO Source

The Release 8 specifications support up to four transmitters and receivers on the eNB, with up to two transmitters and four receivers for the UE. In LTE-Advanced, DL spatial multiplexing of up to eight layers is supported. The Agilent SystemVue W1918 LTE-Advanced library implements a fully-coded DL source with up to eight antennas. Figure 17 shows the component of the LTE-Advanced DL MIMO source.

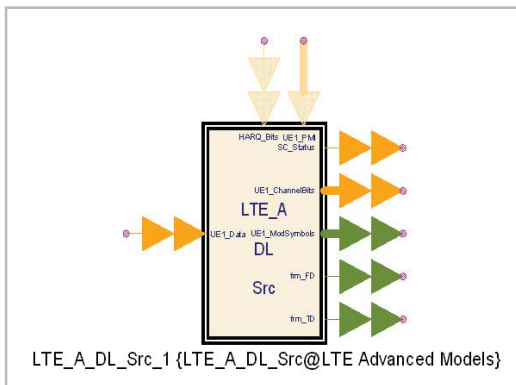


Figure 17. Downlink MIMO Source in the SystemVue LTE-Advanced library

We can open this top-level source and see the detail as shown in Figure 18. Customers can use their own component either with MATLAB or C++ code to replace some SystemVue components for the purpose of verifying their own algorithm.

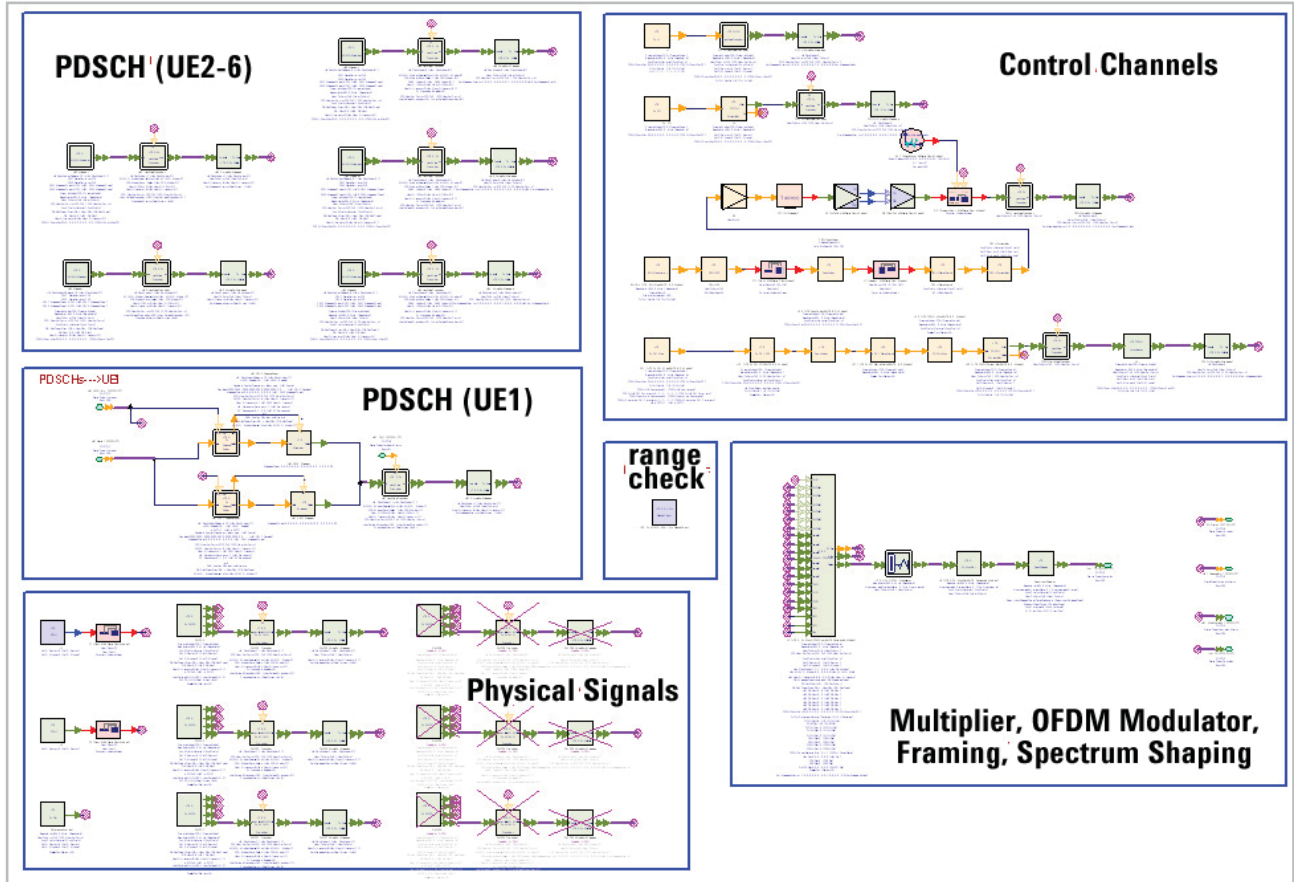


Figure 18. Schematic of LTE-Advanced DL MIMO source, underneath the symbol in Figure 17. This network is parameterized and wrapped under a more convenient GUI, shown in Figures 19-24.

Corresponding to this top-level component, we also develop its GUI to control parameters. The first GUI page, shown in Figure 19, is used to set system parameters (e.g., FDD/TDD, bandwidth and CRS antenna port) of LTE-Advanced.

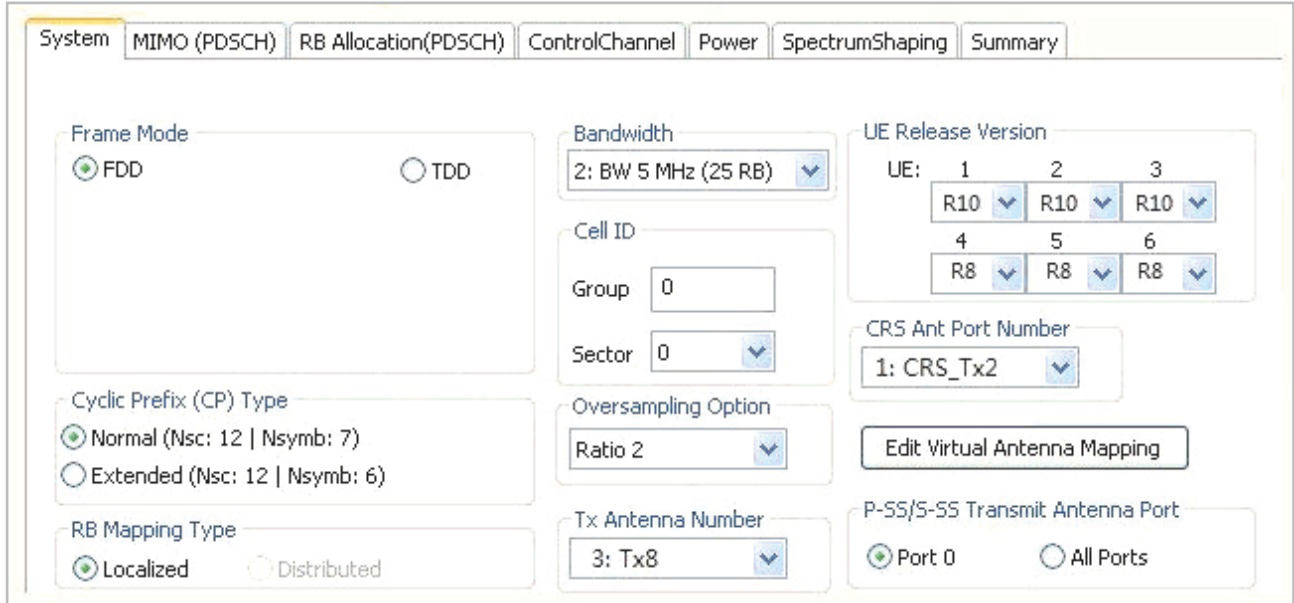


Figure 19. GUI of System parameters for LTE-Advanced DL source

The second GUI page, shown in Figure 20, is used to configure the PDSCH parameters of the MIMO setting (e.g., MIMO mode, number of layers and codebook index) of LTE-Advanced.

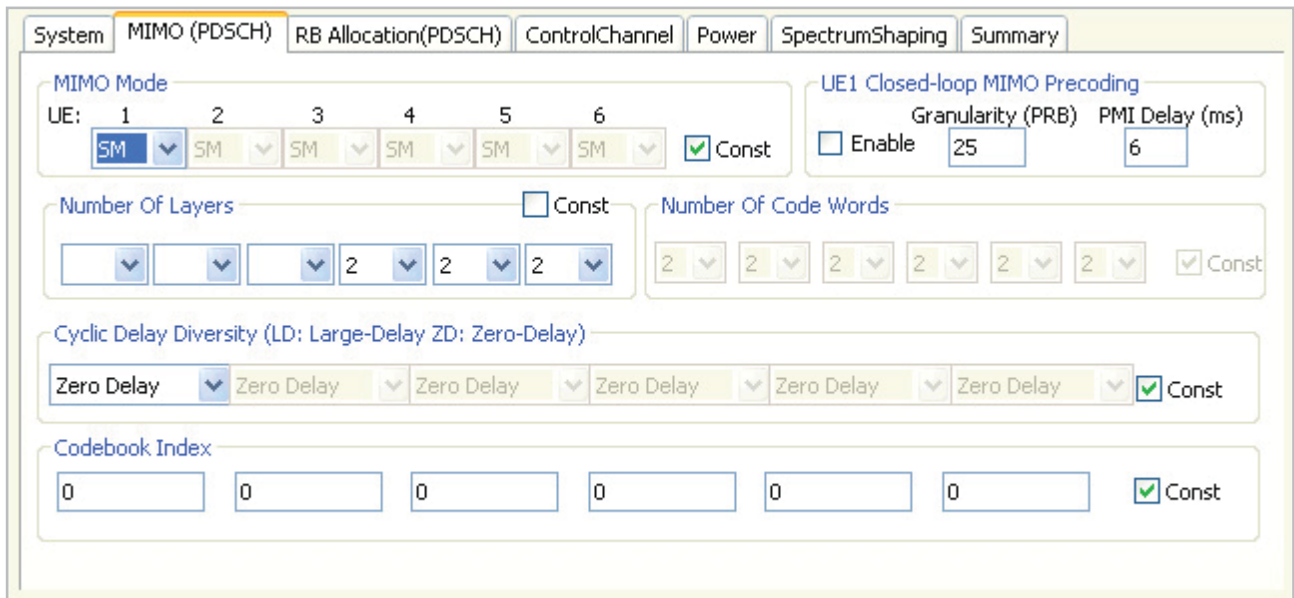


Figure 20. GUI of PDSCH MIMO parameters for LTE-Advanced DL source

The third GUI page, shown in Figure 21 is for PDSCH parameters of RB allocation setting (e.g., resource allocation type, codeword $\frac{1}{2}$ setting of the transport block size, and mapping type) of LTE-Advanced.

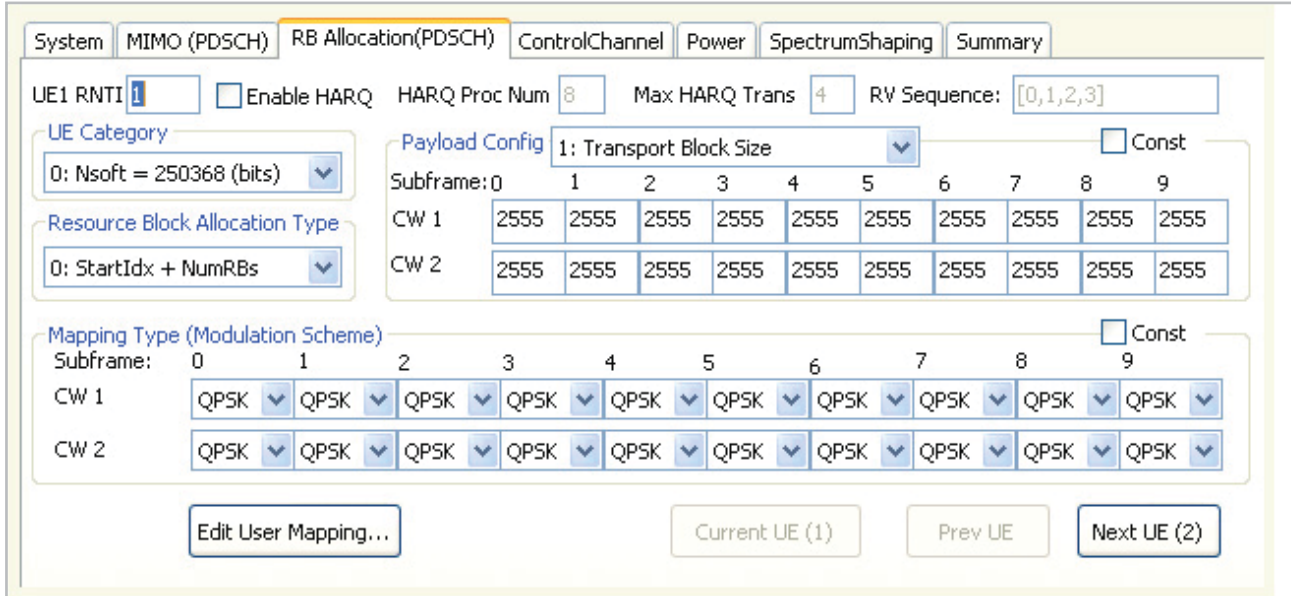


Figure 21. GUI of PDSCH RB allocation parameters for LTE-Advanced DL source

The fourth GUI page, shown in Figure 22, is for control channel setting (e.g., DCI format, PHICH and HARQ setting of LTE-Advanced).

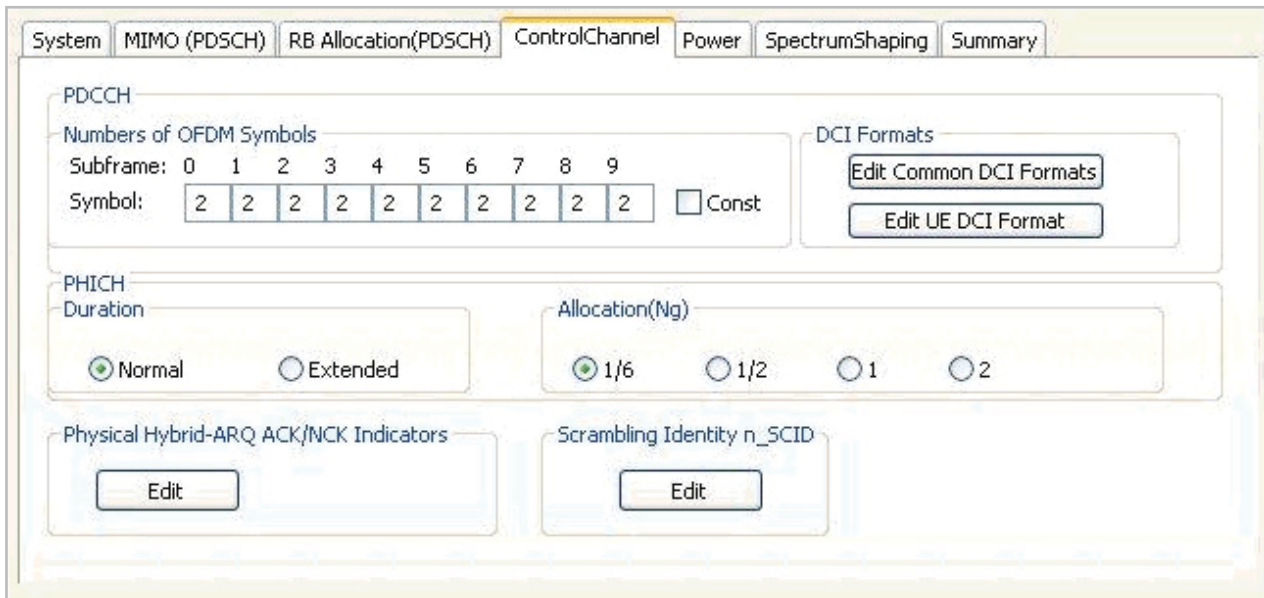


Figure 22. GUI of control channel parameters for LTE-Advanced DL Source

The fifth GUI page, shown in Figure 23, is for power setting (e.g., RS_EPRE, EPRE ratio and PDSCH power ratio) of LTE-Advanced.

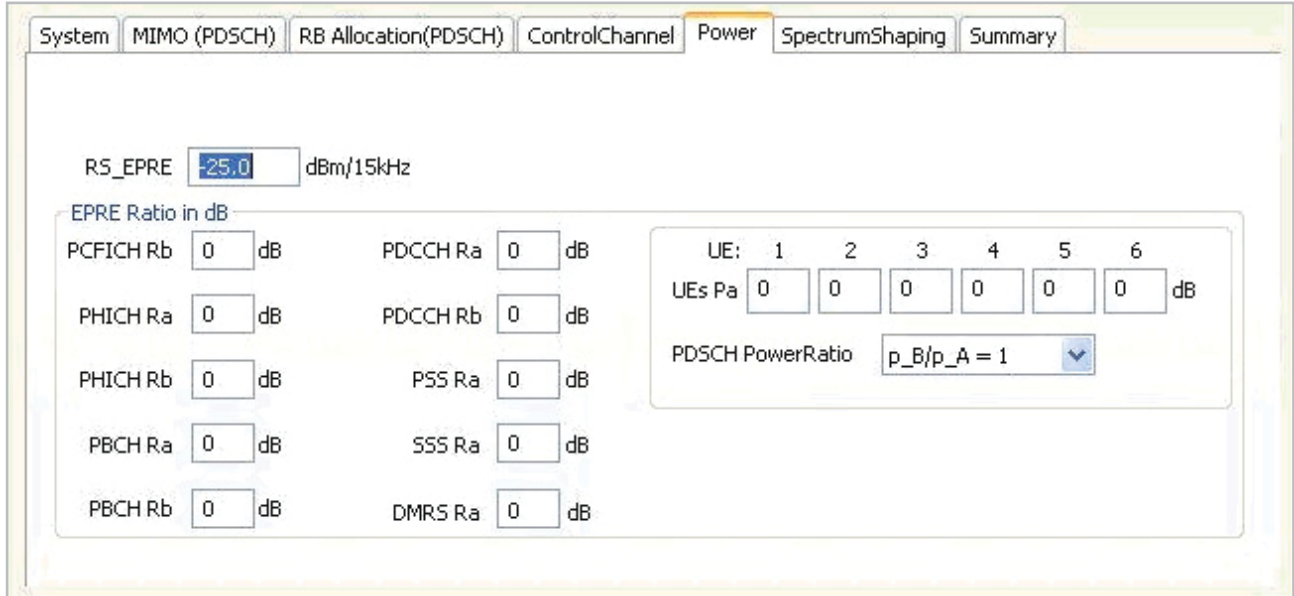


Figure 23. GUI of power parameters for LTE-Advanced DL source

The sixth GUI page, shown in Figure 24, configures the spectrum shaping. Symbol windowing and FIR filtering are provided as spectrum shaping.

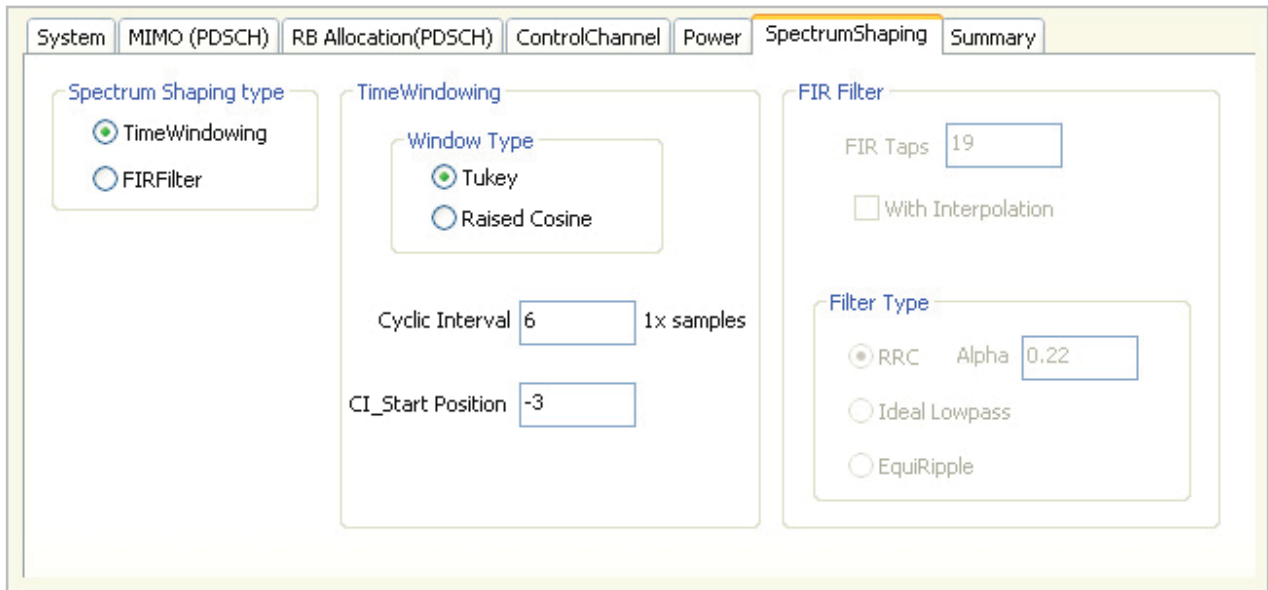


Figure 24. GUI of spectrum shaping parameters for LTE-Advanced DL source

SystemVue LTE-Advanced Uplink MIMO Source

The Release 8 LTE specifications only support single antenna transmission. In LTE-Advanced, UL supports spatial multiplexing MIMO up to 4 layers. SystemVue implements an LTE-Advanced fully-coded UL source up to 4 antennas. Figure 25 shows the component of the LTE-Advanced UL MIMO source.

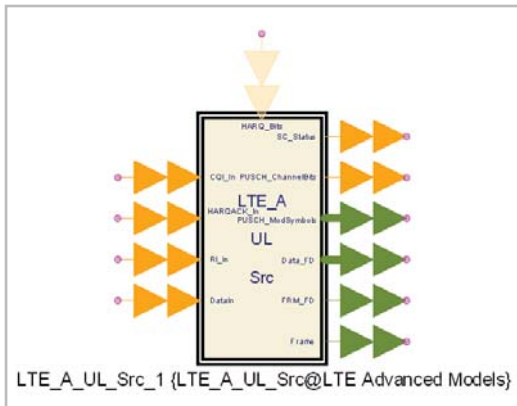


Figure 25. SystemVue LTE-Advanced UL MIMO source

We can open this top-level source and see the underlying detail (Figure 26). Users are free to replace some SystemVue components with their own algorithm components, either as MATLAB or C++ code, to assist in verifying their Release 10 algorithms.

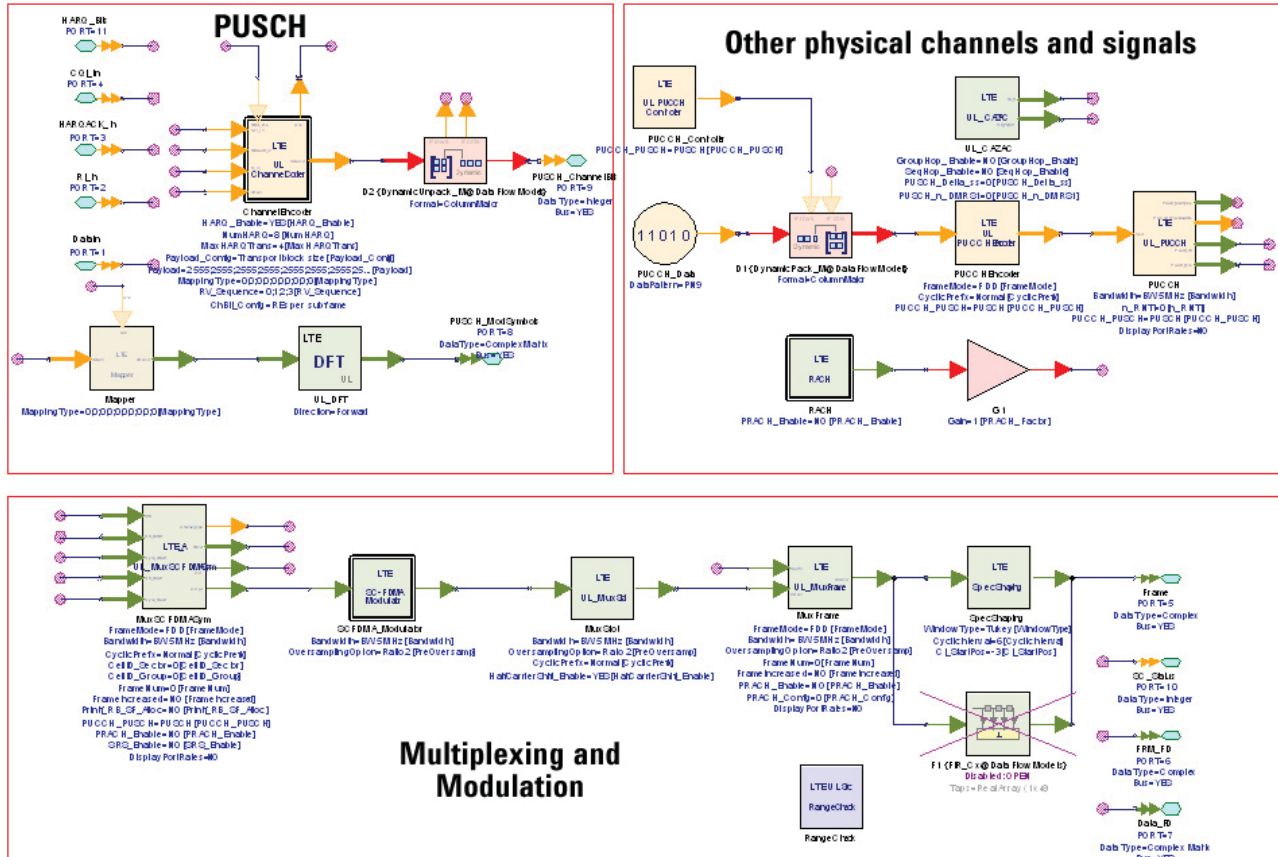


Figure 26. Schematic detail of LTE-Advanced UL MIMO source, shown in Figure 25.

Corresponding to this top-level component, Agilent has also developed a GUI to configure the user-settable parameters. The first GUI page, shown in Figure 27, configures the system parameters (e.g., FDD/TDD and bandwidth) of the LTE-Advanced UL.

The screenshot shows a GUI for configuring LTE-Advanced UL MIMO source parameters. The 'MIMO' tab is selected. The interface is divided into several sections:

- Frame Mode:** Radio buttons for FDD (selected) and TDD.
- Bandwidth:** A dropdown menu showing '2: BW 5 MHz (25 RB)'.
- Cell ID:** Input fields for Group (0) and Sector (0).
- Oversampling Option:** A dropdown menu showing 'Ratio 2'.
- Uplink Specific Config:** Checkboxes for 'Half Subcarrier Shift' (checked), 'Frame Increased', and 'Printf RB Allocation'. Below these are input fields for RNTI (0), Frame Number (0), and a dropdown for Downlink CP (Normal).
- Cyclic Prefix (CP) Type:** Radio buttons for Normal (Nsc: 12 | Nsymb: 7) (selected) and Extended (Nsc: 12 | Nsymb: 6).
- PUCCH/PUSCH Selection:** A dropdown menu showing '0: PUSCH'.

Figure 27. GUI of system parameters of LTE-Advanced UL MIMO source

The third GUI page, shown in Figure 29, is for PUSCH parameters (e.g., DMRS and hopping) of the LTE-Advanced UL.

The screenshot shows a GUI for configuring MIMO parameters of the LTE-Advanced UL MIMO source. The 'MIMO' tab is selected. The interface contains the following parameters:

- Number Of Layers:** A dropdown menu showing '2'.
- Number Of Code Words:** A dropdown menu showing '2'.
- Codebook Index:** An input field showing '0'.

Figure 28. GUI of MIMO parameters of LTE-Advanced UL MIMO source

The third GUI page, shown in Figure 29, is for PUSCH parameters (e.g., DMRS and hopping) of the LTE-Advanced UL.

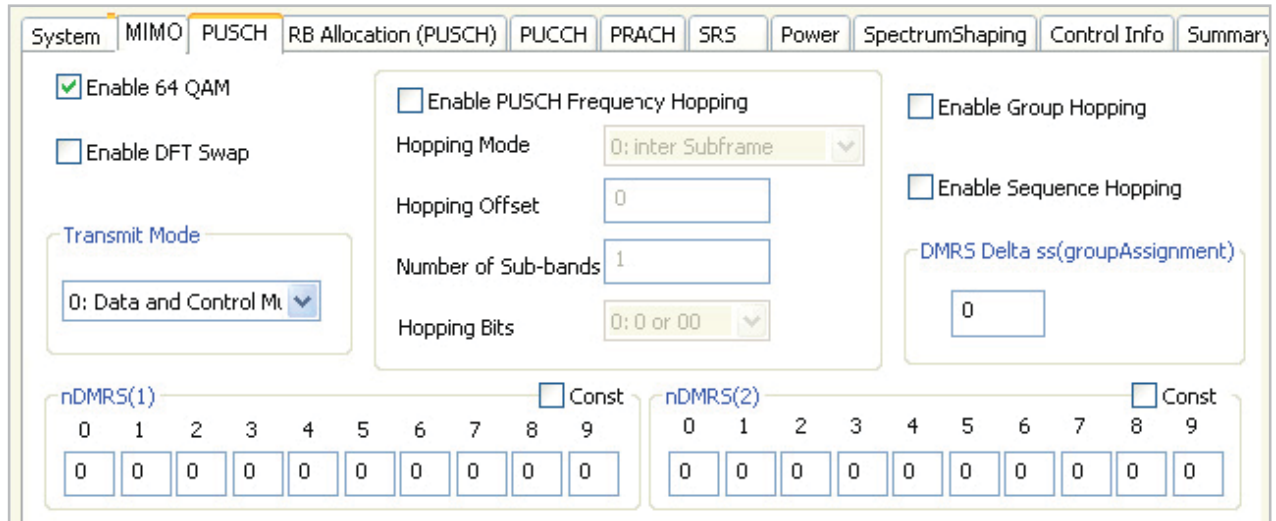


Figure 29. GUI of PUSCH parameters of LTE-Advanced UL MIMO source

The fourth GUI page, shown in Figure 30, is for PUSCH parameters of RB allocation setting (e.g., resource allocation type, codeword ½ setting of transport block size and mapping type) of LTE-Advanced UL.

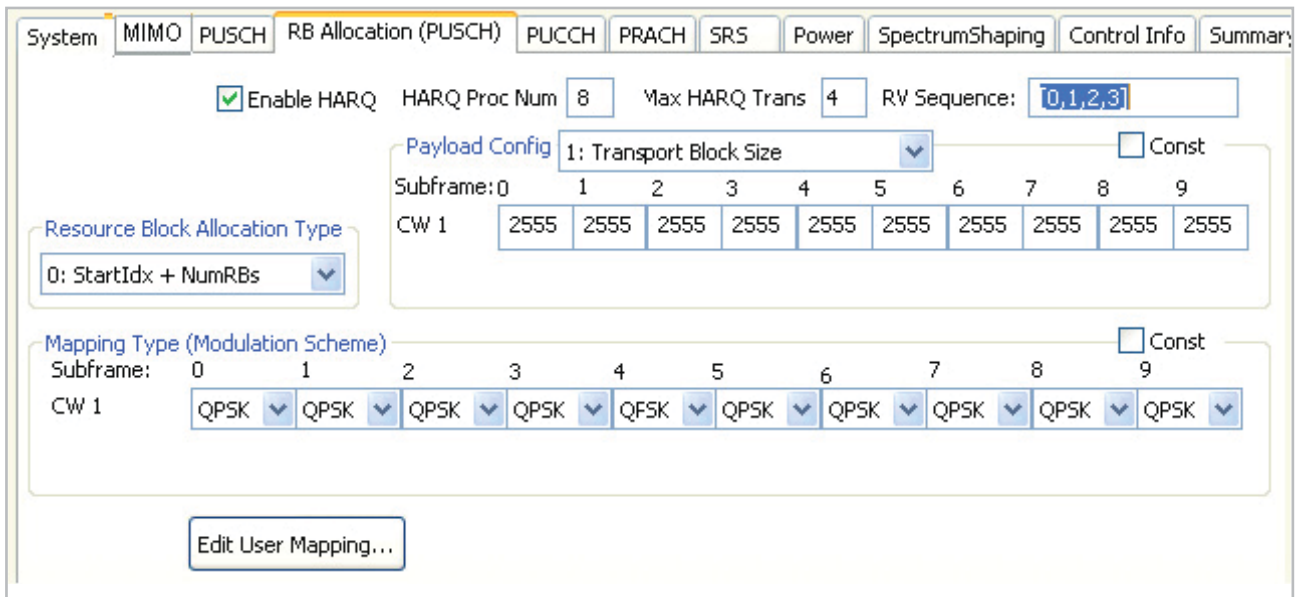


Figure 30. GUI of RB allocation parameters of LTE-Advanced UL MIMO source

The fifth GUI page, shown in Figure 31, is PUCCH parameters setting (e.g., PUCCH format) of LTE-Advanced UL.



Figure 31. GUI of PUCCH parameters of LTE-Advanced UL MIMO source

The sixth GUI page, shown in Figure 32, is for PRACH setting (e.g., preamble index and resource index) of LTE-Advanced UL.

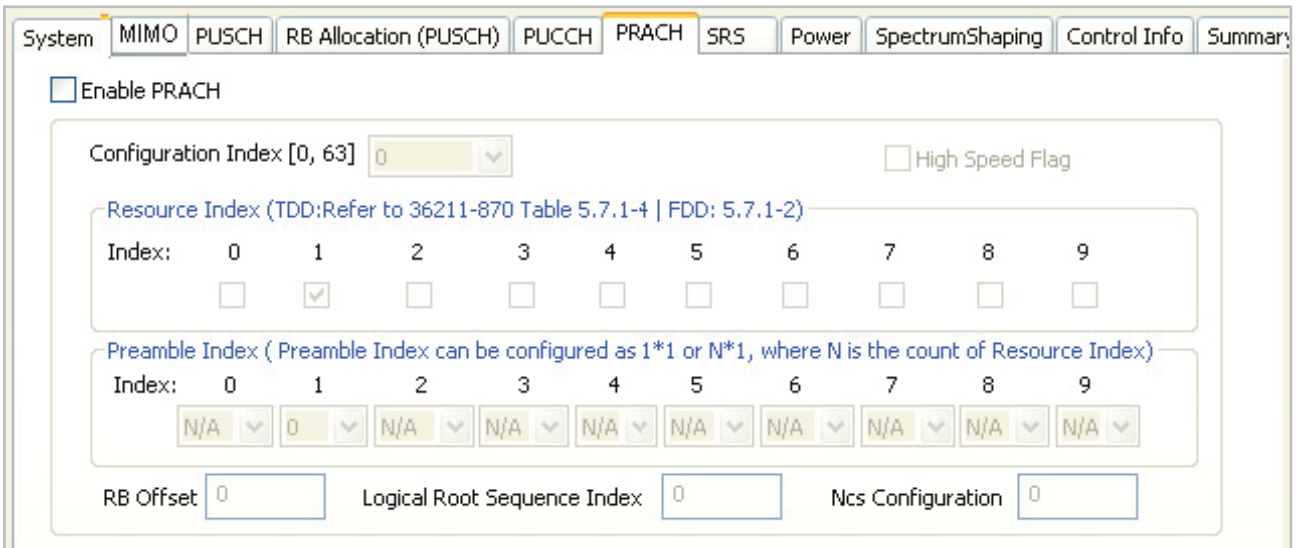
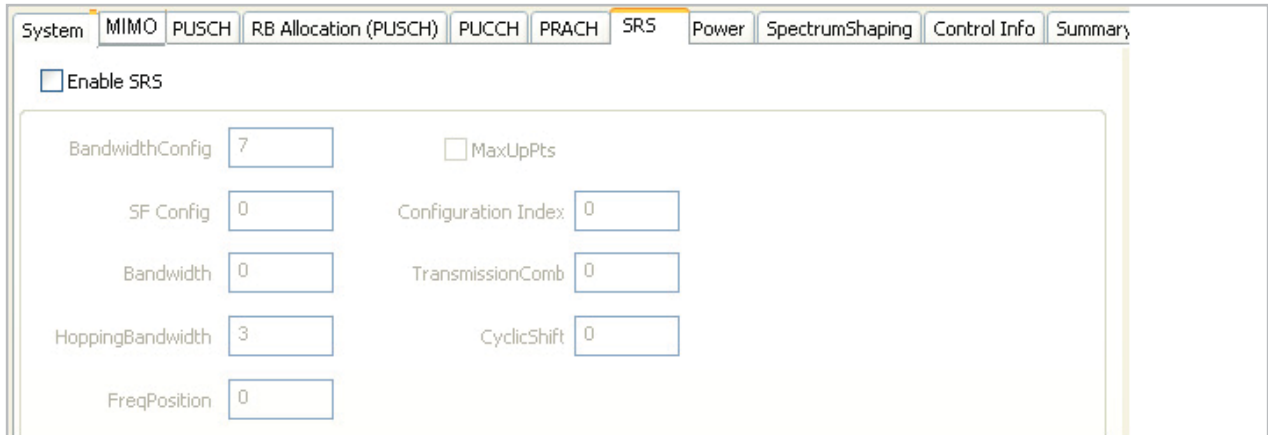


Figure 32. GUI of PRACH parameters of LTE-Advanced UL MIMO source

The seventh GUI page, shown in Figure 33, configures the Sounding Reference Signal (SRS) parameters setting of the LTE-Advanced UL.



System | MIMO | PUSCH | RB Allocation (PUSCH) | PUCCH | PRACH | **SRS** | Power | SpectrumShaping | Control Info | Summary

Enable SRS

BandwidthConfig: MaxUpPts

SF Config: Configuration Index:

Bandwidth: TransmissionComb:

HoppingBandwidth: CyclicShift:

FreqPosition:

Figure 33. GUI of SRS parameters of LTE-Advanced UL MIMO source

The eighth GUI page, shown in Figure 34, configures the UL power parameter setting of the LTE-Advanced UL.



System | MIMO | PUSCH | RB Allocation (PUSCH) | PUCCH | PRACH | SRS | **Power** | SpectrumShaping | Control Info | Summary

PUSCH PowerOffset: dB PUCCH PowerOffset: dB PRACH PowerOffset: dB

PUSCH RS PowerOffset: dB PUCCH RS PowerOffset: dB SRS PowerOffset: dB

Figure 34. GUI of power parameters of LTE-Advanced UL MIMO source

The ninth GUI page, shown in Figure 35, configures the spectrum shaping setting. Symbol windowing and FIR filtering are provided as part of the spectrum shaping parameters.

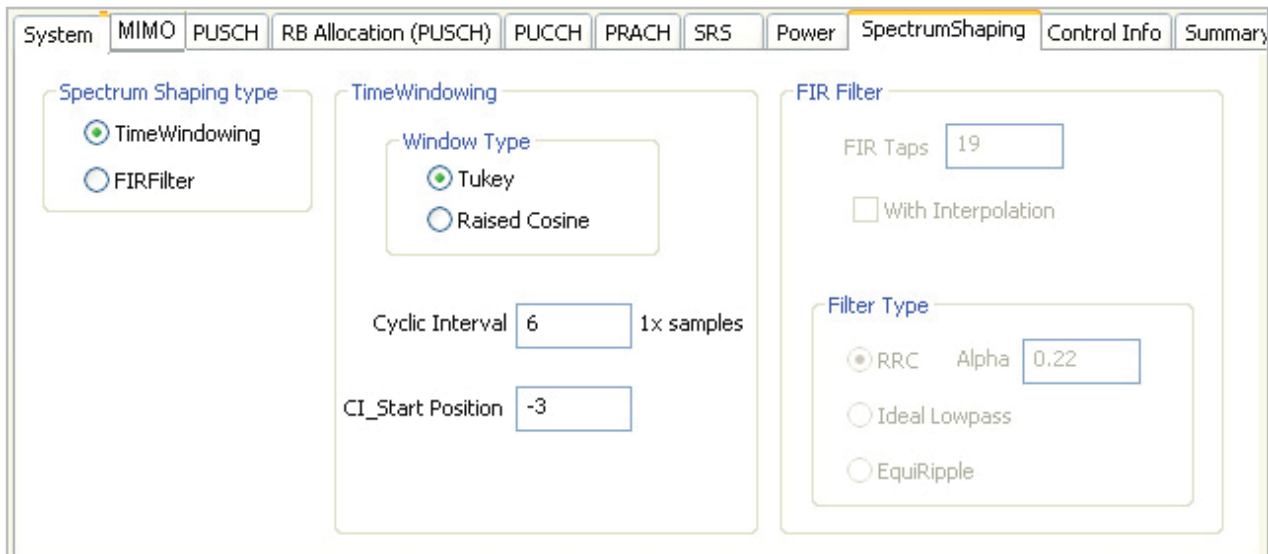


Figure 35. GUI of spectrum shaping parameters of LTE-Advanced UL MIMO source

The tenth GUI page, shown in Figure 36, configures control information (e.g., CQI, RI and ACK/NACK) parameters setting per subframe in the LTE-Advanced UL.

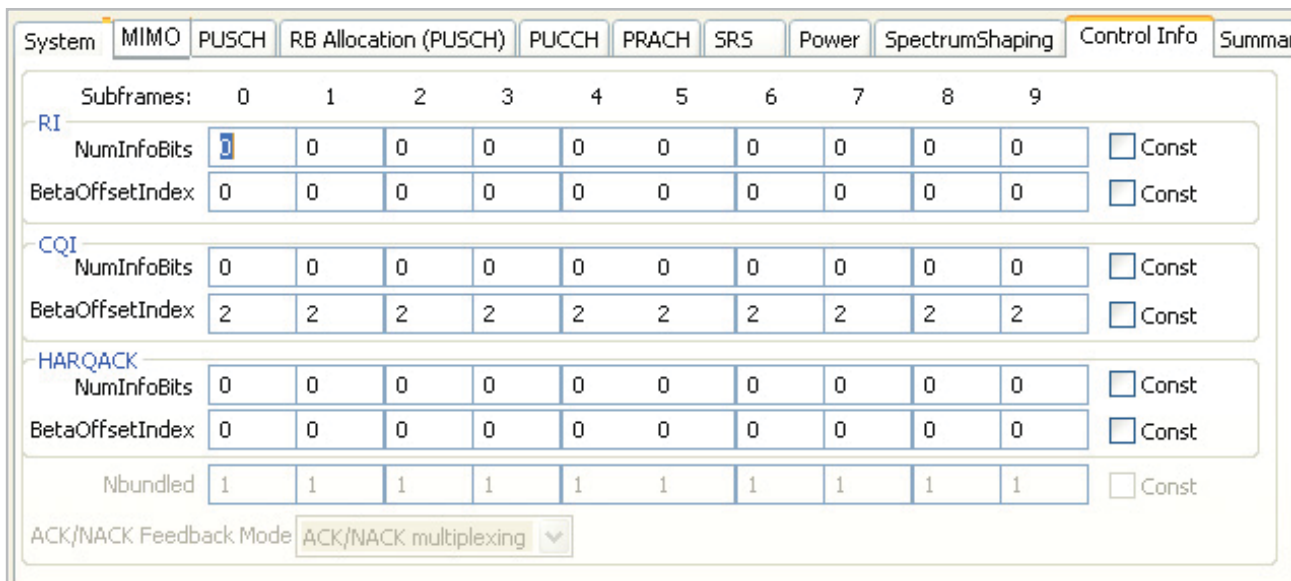


Figure 36. GUI of control information parameters of LTE-Advanced UL MIMO source

SystemVue LTE-Advanced Channel Model

The Agilent SystemVue W1715 MIMO Channel Builder is an optional block set that provides both WINNER II and LTE-Advanced MIMO channel models for BER/BER and throughput fading simulation of LTE, LTE-Advanced, or 802.16m systems. Figure 37 shows an LTE-Advanced MIMO channel model in SystemVue.



Figure 37. LTE-Advanced MIMO channel model in SystemVue

The first GUI page, shown in Figure 38, is to set system parameters, which is consistent with the system simulation conditions, such as carrier frequency and sampling rate.

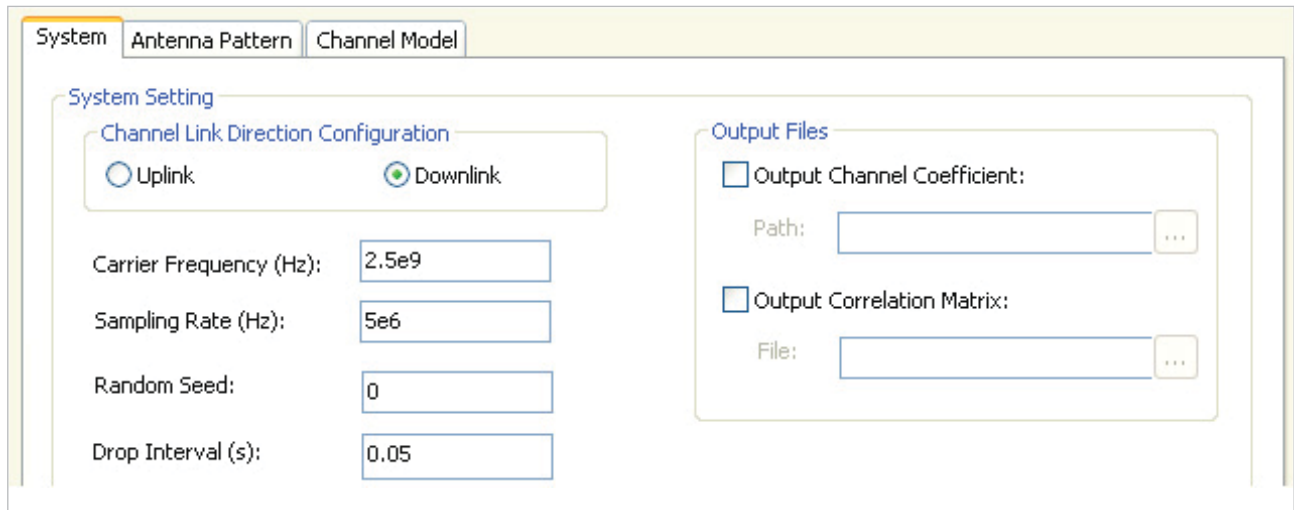


Figure 38. GUI of system parameters for the LTE-Advanced MIMO channel model

The second GUI page, shown in Figure 39, configures the channel model parameters. In the LTE-Advanced MIMO channel model, the channel scenario decides the path parameters. There are four scenarios (InH, Umi, Uma, and RMa) that can be selected from indoor to outdoor environment. The LTE-Advanced channel model is fully consistent with the specifications.

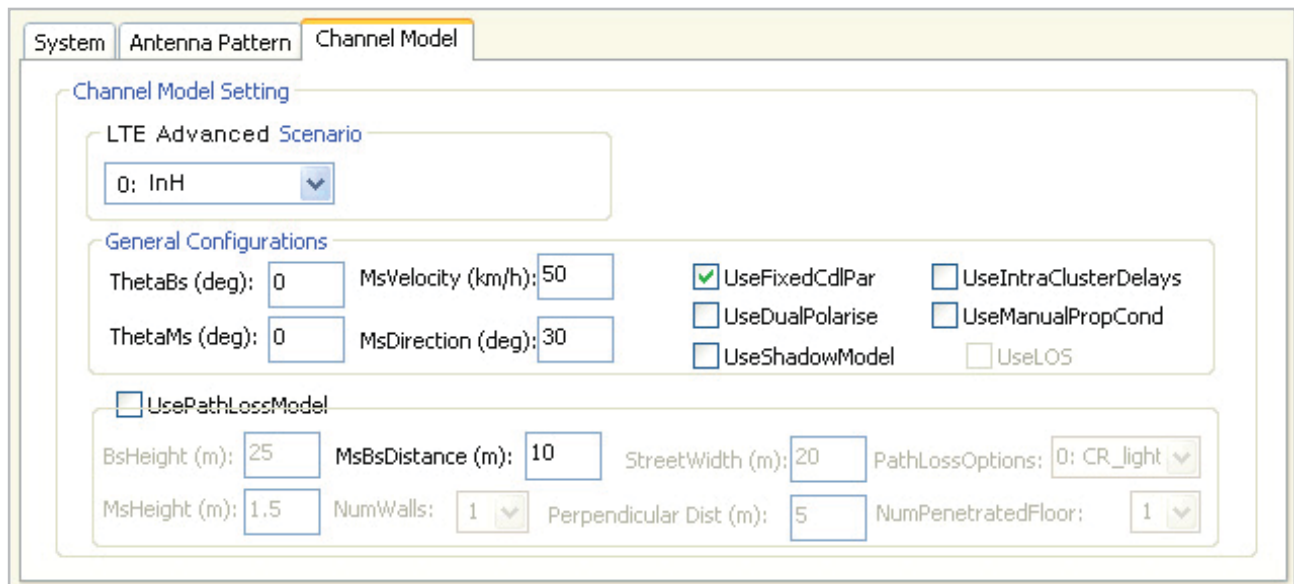


Figure 39. GUI of channel model scenario parameters for LTE-Advanced MIMO channel model

The third GUI page, shown in Figure 40, configures the antenna pattern parameters including orthogonal polarizations (typically linear θ and ϕ polarizations) or farfield radiation patterns simulated by the Agilent EMPro software or other electromagnetic (EM) simulation tools. Ideal antenna patterns such as an omnidirectional pattern, 3-sector pattern and 6-sector pattern are options as well. In the current W1715 MIMO channel builder, both 2D and 3D antenna patterns are considered. Approximate EM wave propagation is regarded as if in one panel, which is widely accepted in channel simulation.

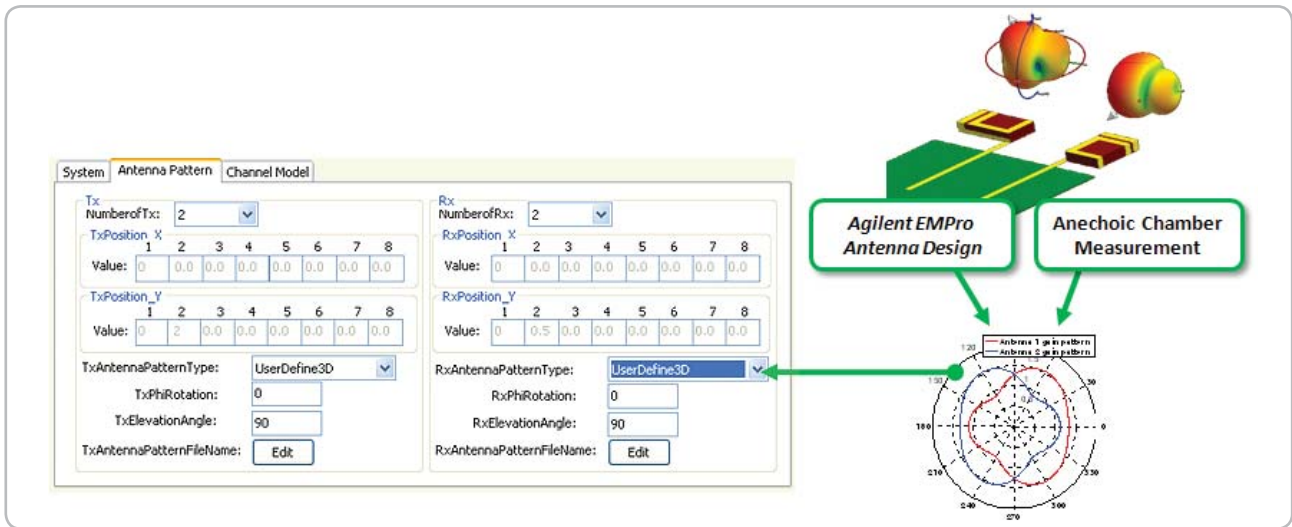


Figure 40. GUI of antenna pattern parameters for LTE-Advanced MIMO channel model

SystemVue LTE-Advanced Carrier Aggregation (CA)

In order to support wider bandwidth in LTE-Advanced, multiple component carriers are combined (carrier aggregation) to provide the necessary bandwidth. In LTE-Advanced, transmission bandwidths up to 100 MHz can be supported through this mechanism.

Two different carrier aggregation techniques have been proposed for LTE-Advanced mobile systems: contiguous CA, when multiple available component carriers are adjacent to each other and non-contiguous CA when they are separated along the frequency band.

TR 36.815 defines deployment scenarios. SystemVue implements three scenarios to characterize spectrum, CCDF and PAPR. Table 10 lists scenario numbers 1, 2 and 4.

Table 10. Deployment scenarios for LTE-Advanced

Scenario no.	Deployment scenario	Transmission BWs of LTE-A carriers	No of LTE-A component carriers	Bands for LTE-A carriers	Duplex modes
1	Single-band contiguous spec. alloc. @ 3.5GHz band for FDD	UL: 40 MHz	UL: Contiguous 2x20 MHz CCs	3.5 GHz band	FDD
		DL: 80 MHz	DL: Contiguous 4x20 MHz CCs		
2	Single-band contiguous spec. alloc. @ Band 40 for TDD	100 MHz	Contiguous 5x20 MHz CCs	Band 40 (2.3 GHz)	TDD
4	Single-band, non-contiguous spec. alloc. @ 3.5GHz band for FDD	UL: 40 MHz	UL: Non-contiguous 1x20 + 1x20 MHz CCs	3.5 GHz band	FDD
		DL: 80 MHz	DL: Non-contiguous 2x20 + 2x20 MHz CCs		

Figure 41 is the schematic for scenario 1, with 4x20MHz FDD DL carrier aggregation in SystemVue. Its spectrum is shown in Figure 42(a). Figure 42(b) is the spectrum of scenario 2, the TDD example.

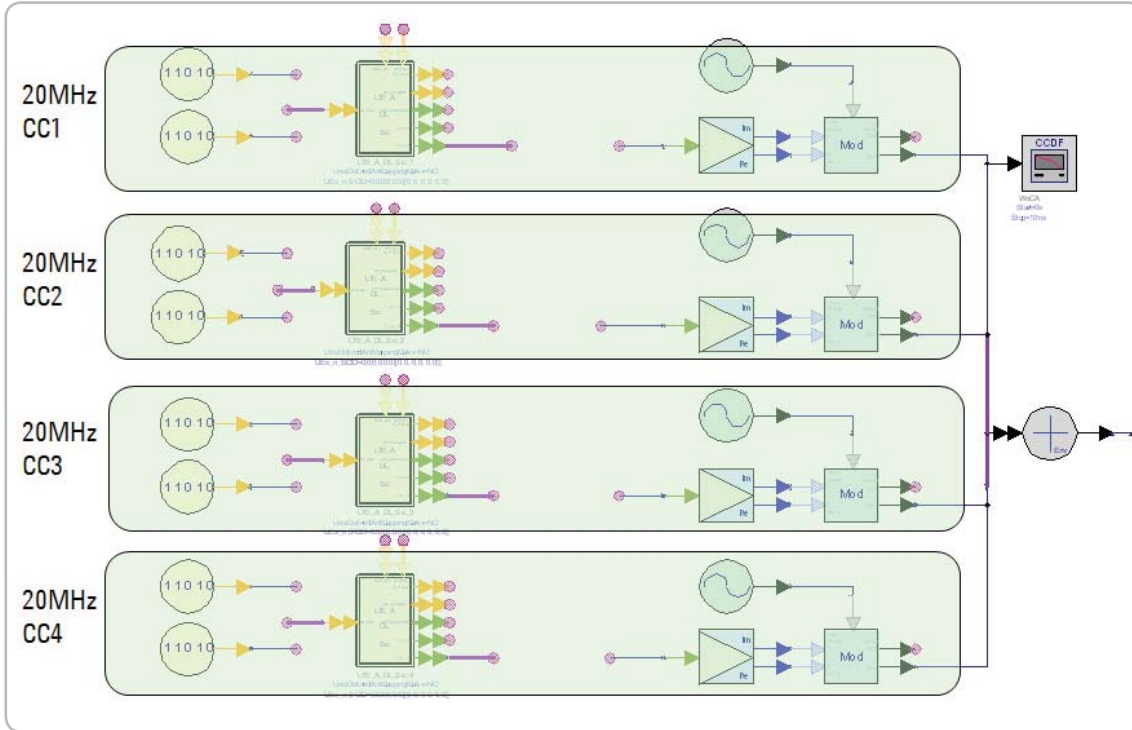


Figure 41. Schematic of scenario 1, 4x20MHz carrier aggregation in SystemVue

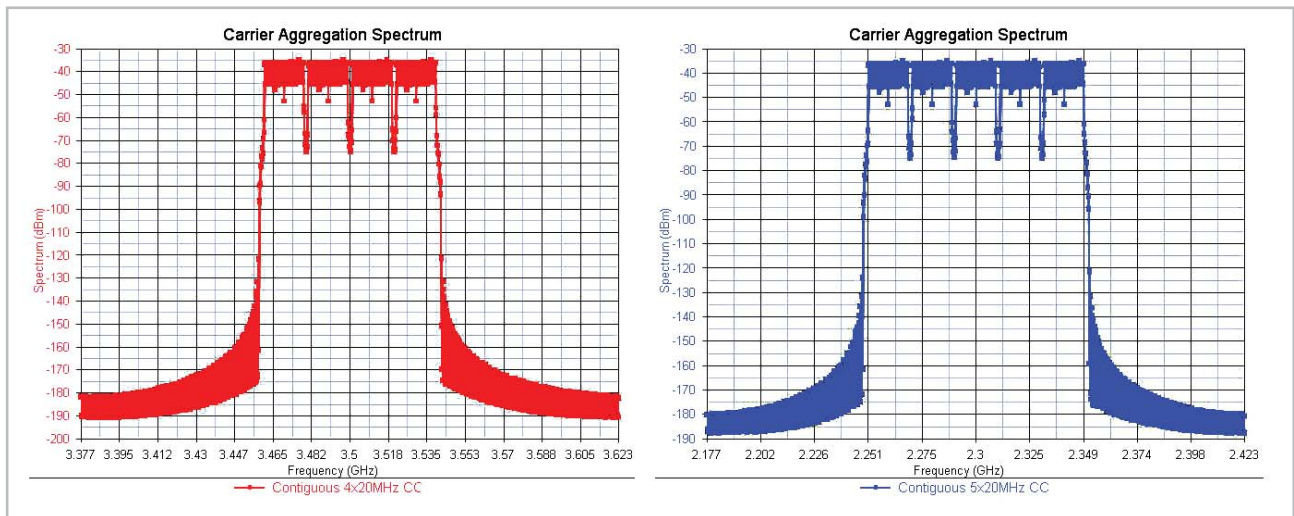


Figure 42. Spectrums of downlink contiguous CCs. (a) is the spectrum of scenario 1 (4x20MHz CCs) and (b) is the spectrum of scenario 2 (5x20MHz CCs)

Scenario 4 is an example of the non-contiguous carrier aggregation case. Figure 43(a) and Figure 43(b) are spectrum of both DL CA and UL CA, respectively.

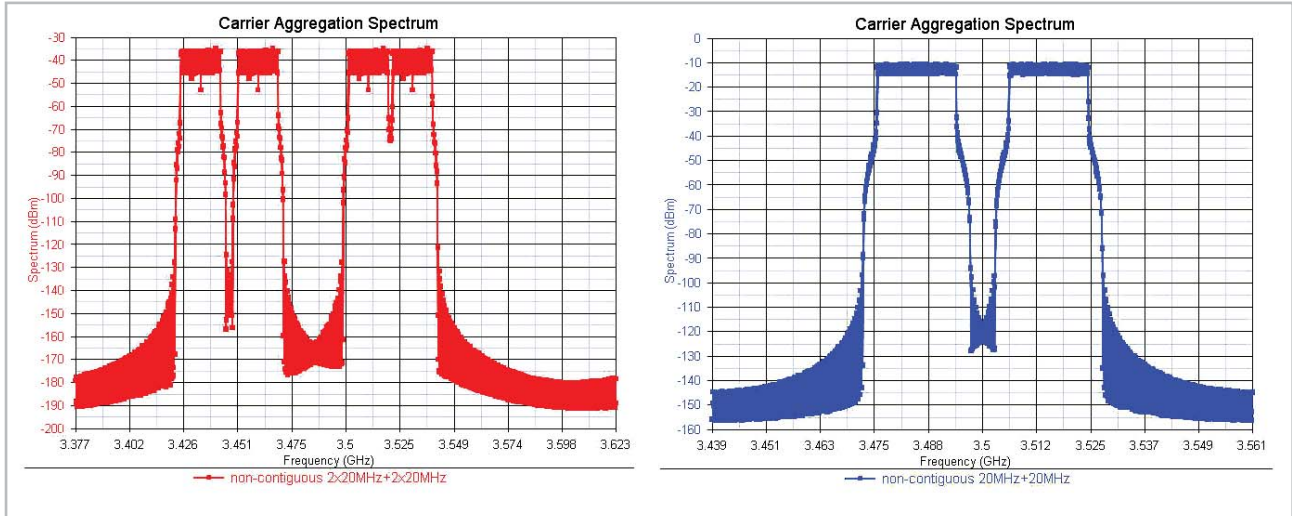


Figure 43. Spectrums of scenario 4 with non-contiguous CCs. (a) is the spectrum of DL (2x20 + 2x20MHz CCs) and (b) is the spectrum of UL (1x20 + 1x20MHz CCs)

When multiple carrier components are transmitted in parallel at both the eNB and UE, the PAPRs of both the eNB and UE increase significantly. Table 11 lists the peak to average power ratio values of the above three CA scenarios.

Table 10. Deployment scenarios for LTE-Advanced

Scenario	Link	Configuration	PAPR of single CC, before aggregation	PAPR with CCs, after aggregation
Scenario 1	FDD DL	4x20 MHz CCs	8.45 dB	9.98 dB
Scenario 2	TDD DL	5x20 MHz CCs	9.17 dB	11.71 dB
Scenario 4	FDD DL	2x20+2x20MHz	8.38 dB	9.58 dB
Scenario 4	FDD UL	20 + 20MHz	5.79 dB	6.86 dB

In a carrier aggregation system, the bandwidth will be up to 100 MHz. The power amplifier (PA) design becomes very important. Moreover, digital pre-distortion (DPD) becomes a key technology. Because of larger PAPR, crest factor reduction (CFR) algorithms need to be investigated for such wideband bandwidth systems. SystemVue has a W1716 digital pre-distortion application kit to deal with LTE-Advanced carrier aggregation. It can provide good performance for PA linearization and is discussed in SystemVue application note 5990-6534EN, among other places.

The challenges for 100MHz terminals include: the potential for a commercial-level RF filter with effective bandwidth range, potential of commercial-level ADC sampling rate, quantization resolution and decoding complexity of channel decoding, and soft buffer size.

SystemVue LTE-Advanced Uplink Enhancement

In LTE-Advanced, DFT-precoded OFDM is the transmission scheme used for PUSCH, both in the presence and absence of spatial multiplexing. In case of multiple component carriers, there is one DFT per component carrier. Both frequency-contiguous and frequency-non-contiguous resource allocation is supported on each component carrier.

Simultaneous transmission of UL L1/L2 control signaling and data is supported through two mechanisms. The control signaling is either multiplexed with data on PUSCH according to the same principle as in Release 8, or transmitted on PUCCH simultaneously with data on PUSCH.

Figure 44 shows the schematic of clustered DFT-S-OFDM of LTE-Advanced in SystemVue.

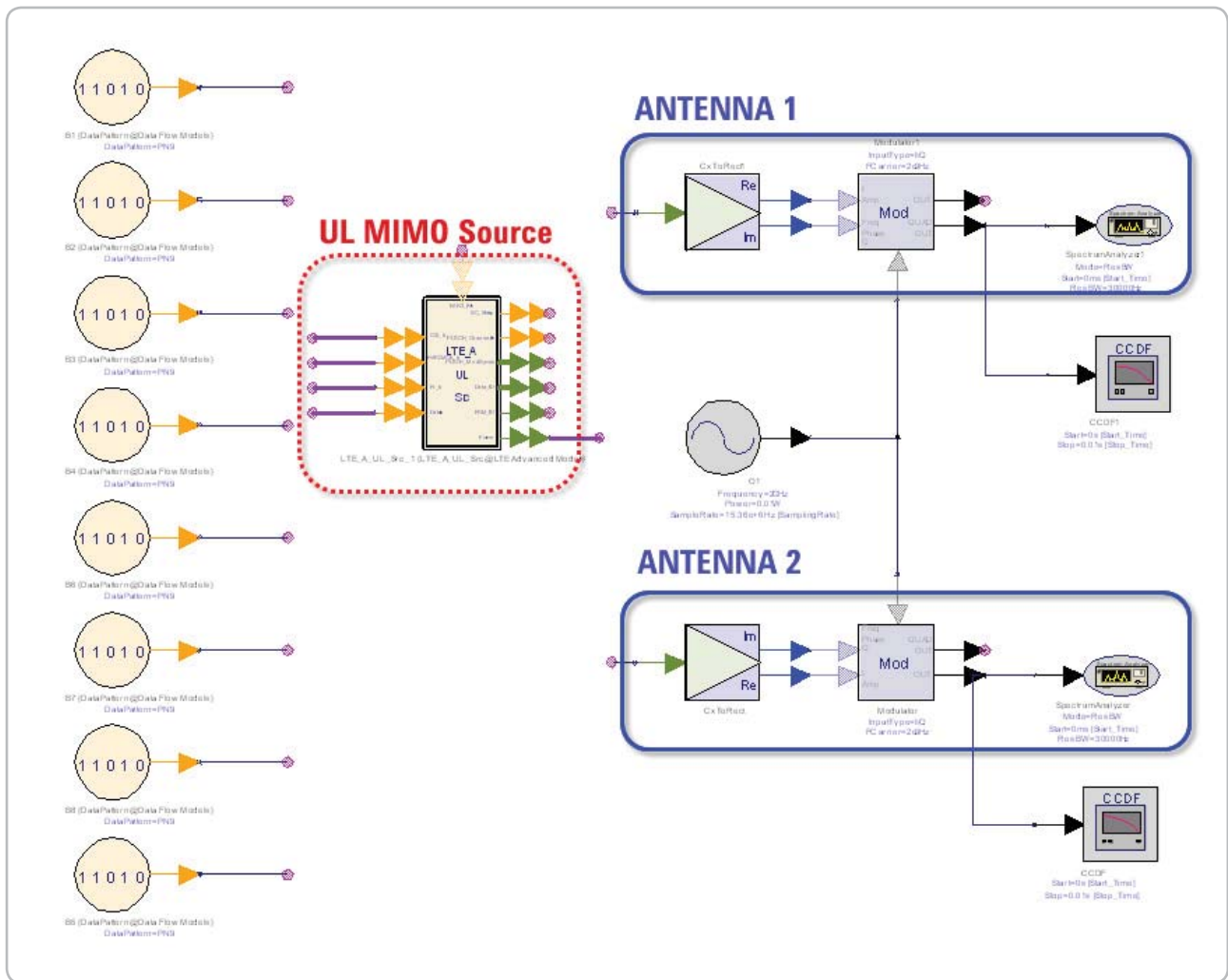


Figure 44. Schematic of clustered DFT-S-OFDM

Figure 45 shows the spectrum of antenna 1. We can see that there are two clustered PUSCHs and PUCCH transmitted simultaneously.

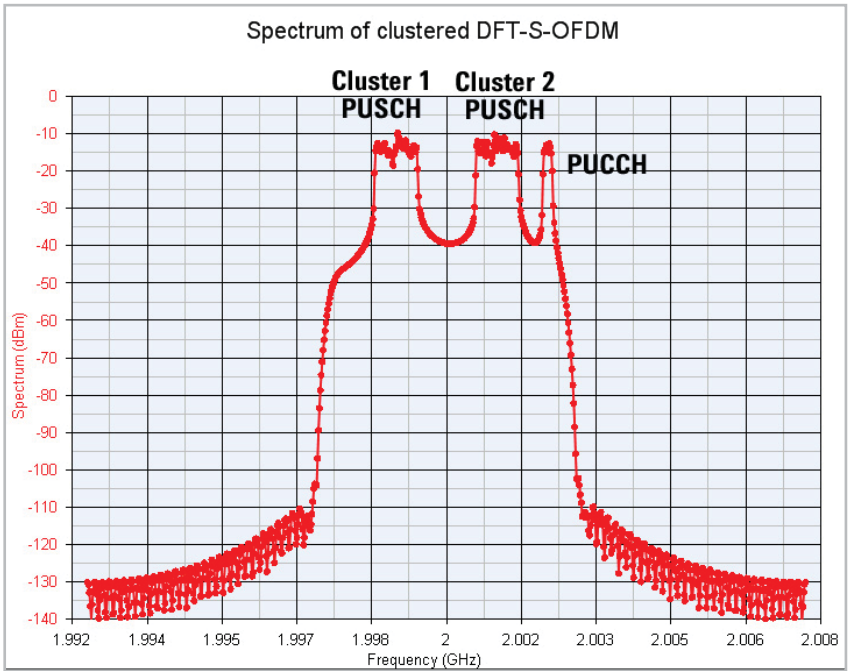


Figure 45. Spectrum of clustered DFT-S-OFDM in SystemVue

SystemVue LTE-Advanced Enhanced MIMO Transmission

SystemVue also provides both DL and UL MIMO receivers, except MIMO sources. Figure 46 presents an example of designing an 8x8 LTE-Advanced system in SystemVue. The closed-loop HARQ throughput is measured as the ACK/NACK and PMI are fed back from the receiver.

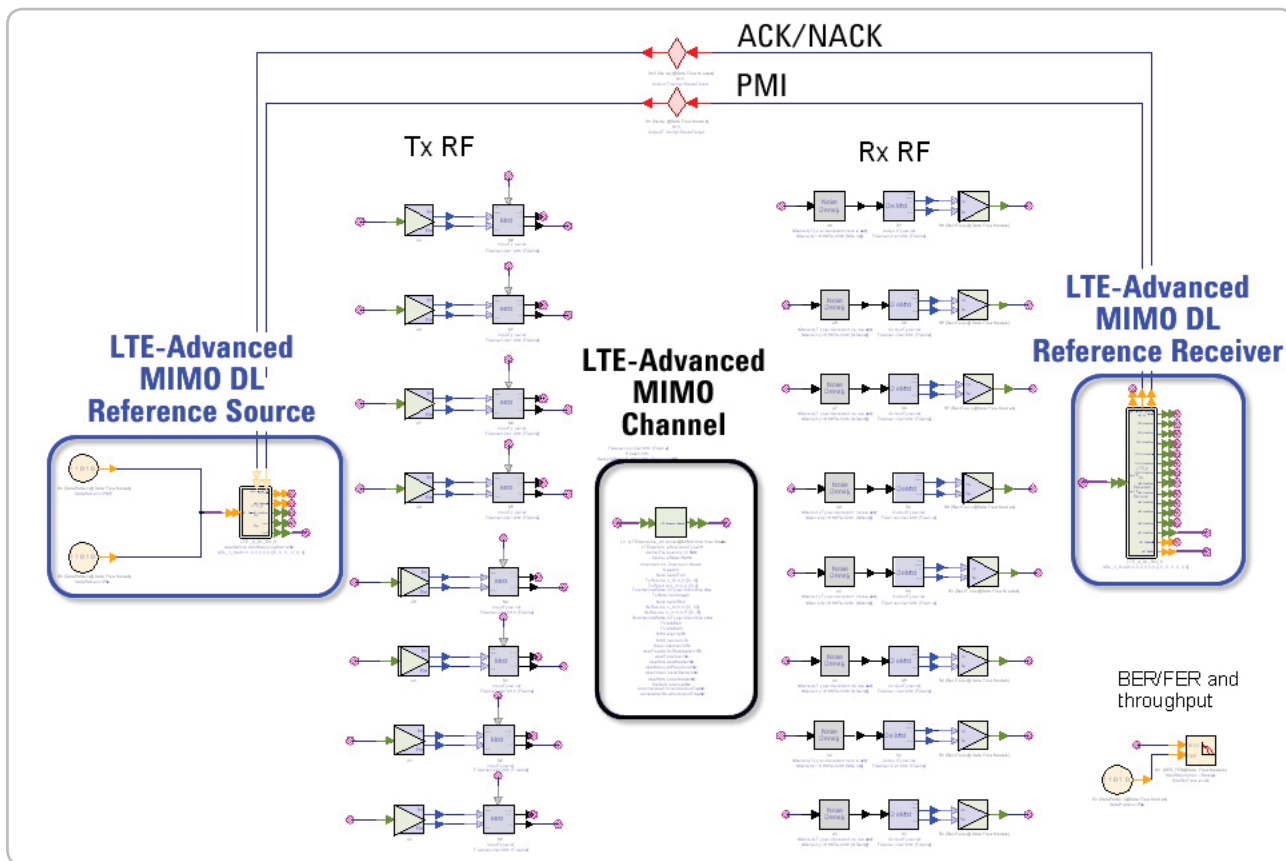


Figure 46. Schematic of the LTE Advanced DL 8x8 MIMO scenario, with fading and closed-loop throughput measurement with active HARQ feedback. SystemVue's "dynamic dataflow" technology is critical for performing this virtual OTA simulation.

LTE-Advanced 8x8 DL throughput simulations require significant computing resources, and even more substantial test equipment requirements, using direct measurement methods. An alternative is shown in the LTE-Advanced DL 2x2 throughput measurement in Figure 47. A Rayleigh radio environment was produced in a chamber by using a multi-probe antenna and channel emulator. Then a two-dipole antenna array with half-wavelength separation was placed at the center of a turntable, and the table oriented at different angles to produce different AoA effects.

The red curve in the figure is the experimental results, which reflects the real world directionality of the antenna array. To measure this trace, an LTE waveform was introduced using a probe antenna, the received data captured from dipole antenna using the Agilent 89600 VSA software, and the captured I/Q data with measured fading saved to a file. The data file was then fed into a simulated reference receiver in SystemVue to complete the throughput results.

The blue curve in Figure 47 represents more purely simulation results. For this curve, a measured antenna pattern file was loaded into SystemVue in lieu of the chamber measurement, and the W1715 MIMO Channel Builder models used in a SystemVue simulation to predict the faded wireless channel with directional MIMO antenna effects. The same simulated reference receiver decoded the results for both measurements.

The simulated MIMO throughput versus the experimental, chamber-based results are compared in Figure 47. Note the small vertical scale, and also that red trace (simulation) is a prediction of the blue trace (measured). This predictive result demonstrated that very early 3DEM simulations of the industrial design of the UE antenna placement (with human SAM models) can be confidently combined with early UE/eNB reference algorithms, and early RF transceiver models to obtain link-level performance, months in advance of actual working UE hardware. While low overall simulation speed permits only a small fraction of Release 10 coverage testing to be practical using simulation tools, nevertheless, key system-level performance parameters can be predicted extremely early in the design process. By integrating these key models and then linking to test equipment as working UE hardware becomes available, Agilent SystemVue helps provide key diagnostic insights about real world performance, possibly saving R&D wafer spins.

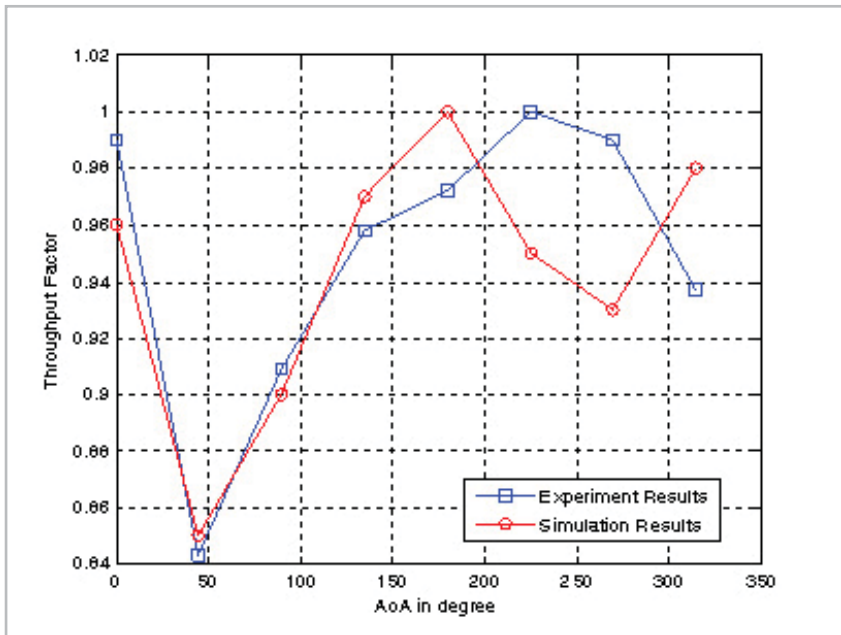


Figure 47. LTE-Advanced throughput vs. Angle of Arrival (AoA), measured vs. simulated results

Summary

In this application note, key techniques and concepts were introduced for LTE, LTE-Advanced, and the LTE-Advanced MIMO channel model. The W1918 SystemVue LTE-Advanced library and enhancements to the W1715 SystemVue MIMO Channel builder were also introduced to enable accurate, predictive, coded throughput results for Release 10.

From these results, it is seen that SystemVue accelerates physical layer algorithm design and product development by providing a configurable, working reference PHY for LTE Advanced. Not shown in this application note, SystemVue can also download simulated waveforms to Agilent signal generators, and receive signals back from Agilent signal analyzers, thus facilitating early R&D validation of working hardware prototypes, for greater insight and confidence. Together, Agilent provides an attractive open modeling platform; leading-edge reference IP; and integration with test equipment, to help you create superior systems designs for emerging standards like LTE-Advanced.

References

1. 3GPP TR 21.905 v9.1.0: "Vocabulary for 3GPP Specifications (Release 9)," 2010-03.
2. 3GPP TS 36.201 v9.1.0: "Evolved Universal Terrestrial Radio Access (E-UTRA); Physical Layer – General Description (Release 9)," 2010-03.
3. 3GPP TS 36.211 v9.1.0: "Evolved Universal Terrestrial Radio Access (E-UTRA); Physical channels and modulation (Release 9)," 2010-03.
4. 3GPP TS 36.212 v9.1.0: "Evolved Universal Terrestrial Radio Access (E-UTRA); Multiplexing and channel coding (Release 9)," 2010-03.
5. 3GPP TS 36.213 v9.1.0: "Evolved Universal Terrestrial Radio Access (E-UTRA); Physical layer procedures (Release 9)," 2010-03.
6. 3GPP TR 36.814 V9.0.0, "Further advancements for E-UTRA physical layer aspects," 2010-03.
7. 3GPP TR 36.815 V9.1.0, "LTE-Advanced feasibility studies in RAN WG4," 2010-06.
8. 3GPP TR 36.912 V9.3.0, "Further Advancements for E-UTRA (LTE-Advanced)," 2010-06.
9. 3GPP TR 36.913 V9.0.0, "Evolved Universal Terrestrial Radio Access (E-UTRA) (LTE-Advanced)," 2009-12.
10. 3GPP TR 36.300 V10.1.0, "Evolved Universal Terrestrial Radio Access (E-UTRA) and Evolved Universal Terrestrial Radio Access Network (E-UTRAN); Overall description; Stage 2 (Release 10)," 2010-09.
11. IST-WINNER II Deliverable 1.1.2 v.1.2, "WINNER II Channel Models," IST-WINNER2, Tech. Rep., 2007 (<http://www.ist-winner.org/deliverables.html>).
12. Introducing LTE-Advanced, <http://cp.literature.agilent.com/litweb/pdf/5990-6706EN.pdf>.
13. Juho Lee, Jin-Kyu Han, and Jianzhong (Charlie) Zhang, "MIMO Technologies in 3GPP LTE and LTE-Advanced," EURASIP Journal on Wireless Communications and Networking, Volume 2009.
14. Stefan Parkvall and David Astely, "The Evolution of LTE towards IMT-Advanced," Journal of Communications, Vol. 4, No. 3, April 2009.
15. Matthew Baker, Chairman 3GPP TSG RAN WG1 "REV-090003r1, LTE-Advanced Physical Layer," Dec 2009.
16. http://www.3gpp.org/ftp/tsg_ran/TSG_RAN/TSGR_50/Docs/RP-101320.zip, Dec 2010.
17. Agilent SystemVue DPD, <http://cp.literature.agilent.com/litweb/pdf/5990-6534EN.pdf>
18. Agilent SystemVue MIMO Channel, <http://cp.literature.agilent.com/litweb/pdf/5990-6535EN.pdf>.

For more information about SystemVue, please visit us on the web:

Product information

<http://www.agilent.com/find/eesof-systemvue>

Product Configurations

<http://www.agilent.com/find/eesof-systemvue-configs>

Request a 30-day Evaluation

<http://www.agilent.com/find/eesof-systemvue-evaluation>

Downloads

<http://www.agilent.com/find/eesof-systemvue-latest-downloads>

Helpful Videos

<http://www.agilent.com/find/eesof-systemvue-videos>

Technical Support Forum

<http://www.agilent.com/find/eesof-systemvue-forum>



Agilent Email Updates

www.agilent.com/find/emailupdates

Get the latest information on the products and applications you select.

www.agilent.com
www.agilent.com/find/eesof-systemvue-lte-advanced

For more information on Agilent Technologies' products, applications or services, please contact your local Agilent office. The complete list is available at:

www.agilent.com/find/contactus

Americas

Canada	(877) 894 4414
Brazil	(11) 4197 3500
Mexico	01800 5064 800
United States	(800) 829 4444

Asia Pacific

Australia	1 800 629 485
China	800 810 0189
Hong Kong	800 938 693
India	1 800 112 929
Japan	0120 (421) 345
Korea	080 769 0800
Malaysia	1 800 888 848
Singapore	1 800 375 8100
Taiwan	0800 047 866
Other AP Countries	(65) 375 8100

Europe & Middle East

Belgium	32 (0) 2 404 93 40
Denmark	45 70 13 15 15
Finland	358 (0) 10 855 2100
France	0825 010 700*
	*0.125 €/minute
Germany	49 (0) 7031 464 6333
Ireland	1890 924 204
Israel	972-3-9288-504/544
Italy	39 02 92 60 8484
Netherlands	31 (0) 20 547 2111
Spain	34 (91) 631 3300
Sweden	0200-88 22 55
United Kingdom	44 (0) 118 9276201

For other unlisted Countries:

www.agilent.com/find/contactus

Revised: October 14, 2010

Product specifications and descriptions in this document subject to change without notice.

© Agilent Technologies, Inc. 2010
Printed in USA, December 23, 2010
5990-7146EN



Agilent Technologies